4 Country Report: France

Executive Summary

The Montreal Protocol (1987) and Kyoto Protocol (1997), alongside the European F-Gas Regulation (2006, revised in 2014), and more recently, the Kigali Amendment to the Montreal Protocol (2016), mandate a transition toward refrigerants possessing zero ozone depletion potential and significantly reduced Global Warming Potential (GWP). This regulatory framework implies the gradual phasing out of hydrofluorocarbons (HFCs) in favor of 4th generation refrigerants, such as HFC/HFO blends, pure HFOs (olefins), or "natural" refrigerants (hydrocarbons, CO_2, NH_3, H_2O, etc.).

Specifically, within Europe, the F-Gas regulation enforces a schedule for reducing CO2 emissions associated with refrigerant use (via phase-down of market quotas). It prohibits selling some of the high GWP HFCs (e.g., R404A). By 2020, marketing quotas have already been reduced by 37%, with a continued reduction until 2030, reaching 79%. Consequently, existing HFCs will phase out, prompting manufacturers to explore new refrigerants characterized by low GWP (< 150), often flammable, potentially impacting product design, sizing, and energy efficiency.

Refrigerants commonly employed in residential heat pumps, air conditioners, and thermodynamic water heaters include R410A, R407C, and R134a, with respective Global Warming Potentials (GWPs) of 2088, 1650, and 1430, subject to regulation under the F-Gas directive. Presently, alternative solutions with low GWPs (< 150) for R407C (such as R455A or R454C) and R134a (such as R1234yf, R1234ze(E)) are known, reflecting current understanding. However, replacing R410A presents challenges since no refrigerant with a GWP below 150 is currently commercially available.

The challenges in this context are:

- Replacing HFC refrigerants, characterized by a high global warming potential (GWP) (> 2500), which are non-toxic and non-flammable (class A1), with low GWP alternatives (< 150), which are generally non-toxic but often flammable (class A2L, A2 or A3).
- Development of products within the regulatory framework (F-Gas and national regulations concerning flammability), requiring the maintenance of energy performance levels at least equivalent to existing standards.

The project aims to achieve the following objectives:

- Assisting manufacturers in transitioning away from HFCs, ensuring viable alternatives are available by 2030.
- Facilitating the adoption of (highly) flammable fluids while adhering to regulatory requirements.

4.1 Design and study of a prototype of heat pump using 150 g of propane

Prepared by: Alexandre ROYER[1*]

[1]CETIAT, Centre Technique des Industries Aérauliques et Thermiques, HVAC Systems Department, Villeurbanne, France

***Corresponding author e-mail: alexandre.royer@cetiat.fr**

4.1.1 Introduction

This report presents a study carried out by CETIAT on the use of low GWP refrigerant in heat pumps and more specifically on the use of propane as refrigerant.

The progressive phase-out of HFCs and their replacement by natural flammable fluid requires reducing the charge of refrigerant in heat pumps. The objective of this study was to develop a heat pump with the minimum amount of propane possible for an individual 5-kW residential space heating application. An experimental water-to-brine heat pump prototype was built and tested. The unit was designed to be compatible with outdoor air to brine heat exchanger.

The study first focuses on the influence of gas superheating entering the compressor and compressor speed during charge optimisation. It secondly analyses the influence of different evaporator sizes, condenser sizes and compressor technologies on the optimal propane charge. Finally, a seasonal performances analysis is performed on two configurations for which the optimal charges are 190 g and 90 g, respectively.

To answer low GWP restriction, new refrigerants with low GWP are now offered by the chemical industry and natural fluid as propane are the subject of many studies. As propane has flammable properties (A3 classification), a common safety measure is to reduce the refrigerant charge to its minimum while avoiding impacting the performance negatively. In this context, a water-to-water heat pump appears to be the configuration with the smallest internal volume and thus the smallest charge amount. Those units are widely used for ground sourced applications. However, ground sourced units require drillings or buried water pipes which are not available options in every case. That is why the experimental 5- kW heat pump built for this study is a water-to-brine unit, compatible with outdoor air to brine heat exchanger.

Such a unit can be placed inside a house with a maximum admissible charge of propane of 150 g.

The objectives of this work are to assess experimentally the minimum charge of propane for a 5-kW water to brine heat pump and to evaluate the influence of different parameters and component on the optimal charge amount.

The report is divided into two parts:1) presentation of the prototype and the test campaign; 2) analysis of the results and conclusions.

4.1.2 Prototype

For this study, a prototype was built following the diagrams showed in Figure 4-1.

The choice of the components and the details of the test campaign were based on the following constraints:

- Average climate heat pump;
- Bivalence temperature of -10 °C;
- Design capacity of 5 kW;
- Medium temperature application of 55 °C;
- Use of water/glycol mixture (MPG40, 40 % monopropylene glycol) at the source side.

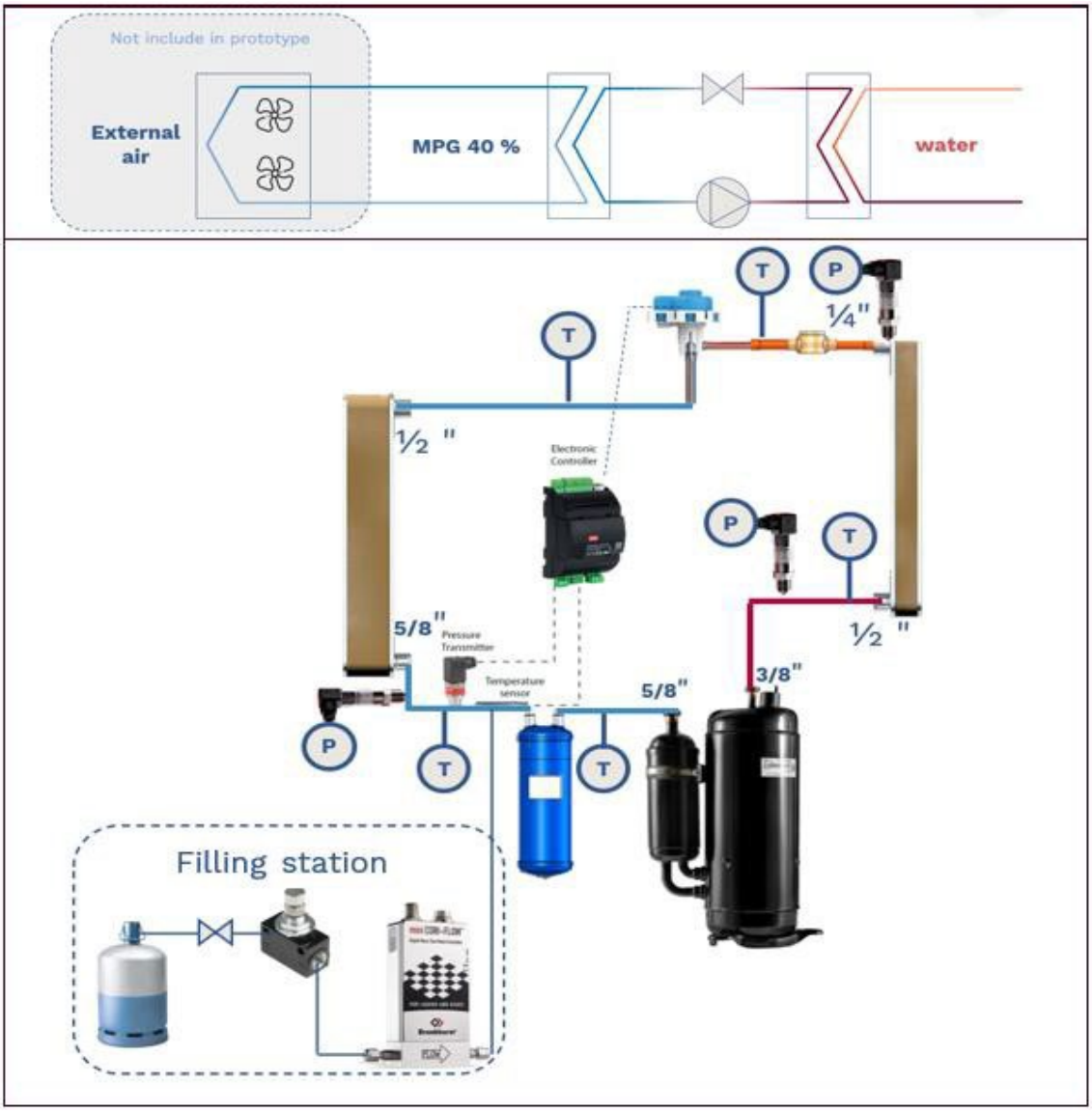

Figure 4-1: Prototype layout

These constraints are fixed. Table 4-1 shows the component selection summary and Table 2 shows the test plan allowing to study:

- The impact of different parameters on the optimal charge of propane:
  i) Superheating at the compressor inlet;
  ii) Compressor speed;
  iii) Heat exchangers size;
  iv) Compressor technology.
- The impact of the compressor technology on seasonal performance (adapted from standard EN 14825)

Table 4-1: Components selection summary

Component	Type
Compressor 1	Rotary 30.6 cc Hermetic; Oil: 870 mL PAG (XS-601C1)
Compressor 2	Scroll 33 cc; Semi-hermetic automotive Oil: 150 g PAG (SP-A2)
Evaporator	Dimple plates; 20 plates / 30 plates / 40 plates
Condenser	Dimple plates; 20 plates / 30 plates

Table 2: Test campaign

				Refrigerant charge optimization		Seasonal performances (adapted from EN 14825)
	Compressor	Evaporator	Condenser	Frq (Hz)	Superheating (K)	
Conf. 1	rotary	30 p.	20 p.	60	5, 10, 15	
				25	10	
				90	10	
Conf. 2	rotary	40 p.	20 p.	60	10	NO
Conf. 3	rotary	20 p.	20 p.	60	10	YES
Conf. 4	scroll	20 p.	20 p.	60	10	YES
Conf. 5	scroll	20 p.	30 p.	60	10	NO

Then, the test conditions were chosen according to EN 14511 and EN 14825, considering the hypothesis of an air-to-water heat pump with a thermal pinch of 3 °C in the air-to-brine heat exchanger. This value can be modified in case of a minimum flow or ON/OFF cycling as described in the standards. These conditions are summarized in Table 3 below.

Table 3: Test conditions

	Air-to-brine heat exchanger (outdoor)		Brine heat exchanger (intermediary circuit)		Water heat exchanger (indoor)	
	Dry air temperature	Wet air temperature	Inlet temperature	Outlet temperature	Inlet temperature	Outlet temperature
Nominal conditions	7 °C	6 °C	4 °C	-1 °C	47 °C	55 °C
SCOP A	- 7 °C	- 8 °C	-10 °C	-15 °C	44 °C	52 °C
SCOP B	2 °C	1 °C	-1 °C	-6 °C	34 °C	42 °C
SCOP C	7 °C	6 °C	4 °C	-1 °C	28 °C	36 °C
SCOP D	12 °C	11 °C	9 °C	4 °C	22 °C	30 °C
SCOP E/F	- 10 °C	- 11 °C	-13 °C	-18 °C	47 °C	55 °C

Figure 4-2 and Figure 4-3 show the heat pump prototype and the experimental setup.

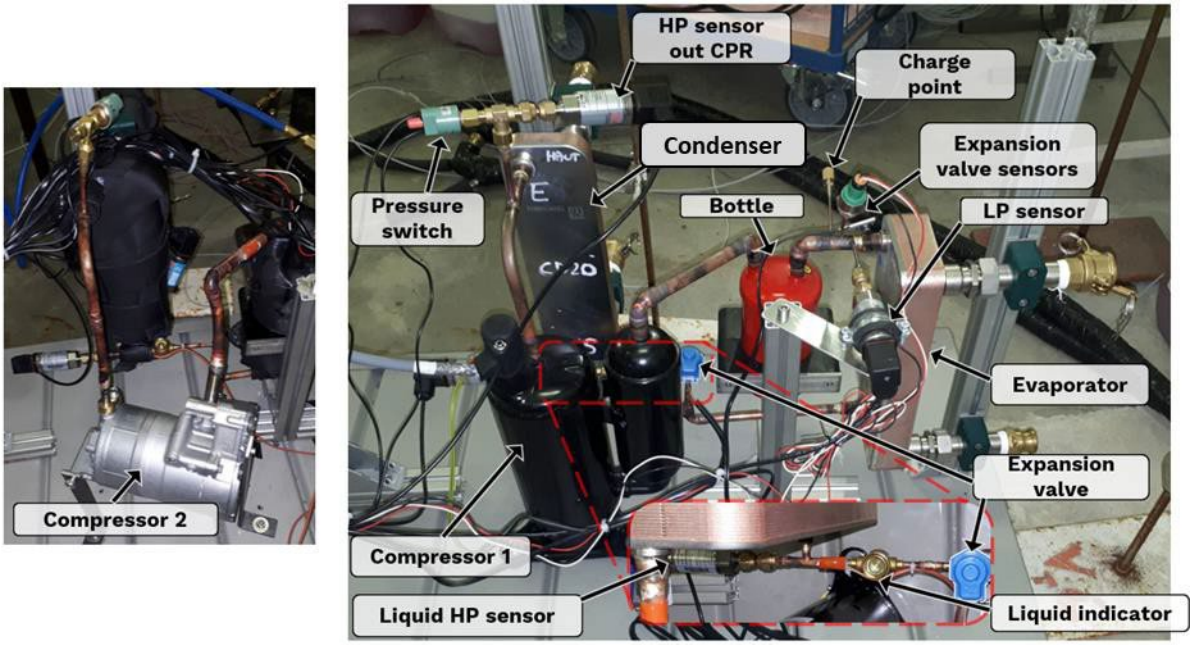

Figure 4-2: Photo of the prototype

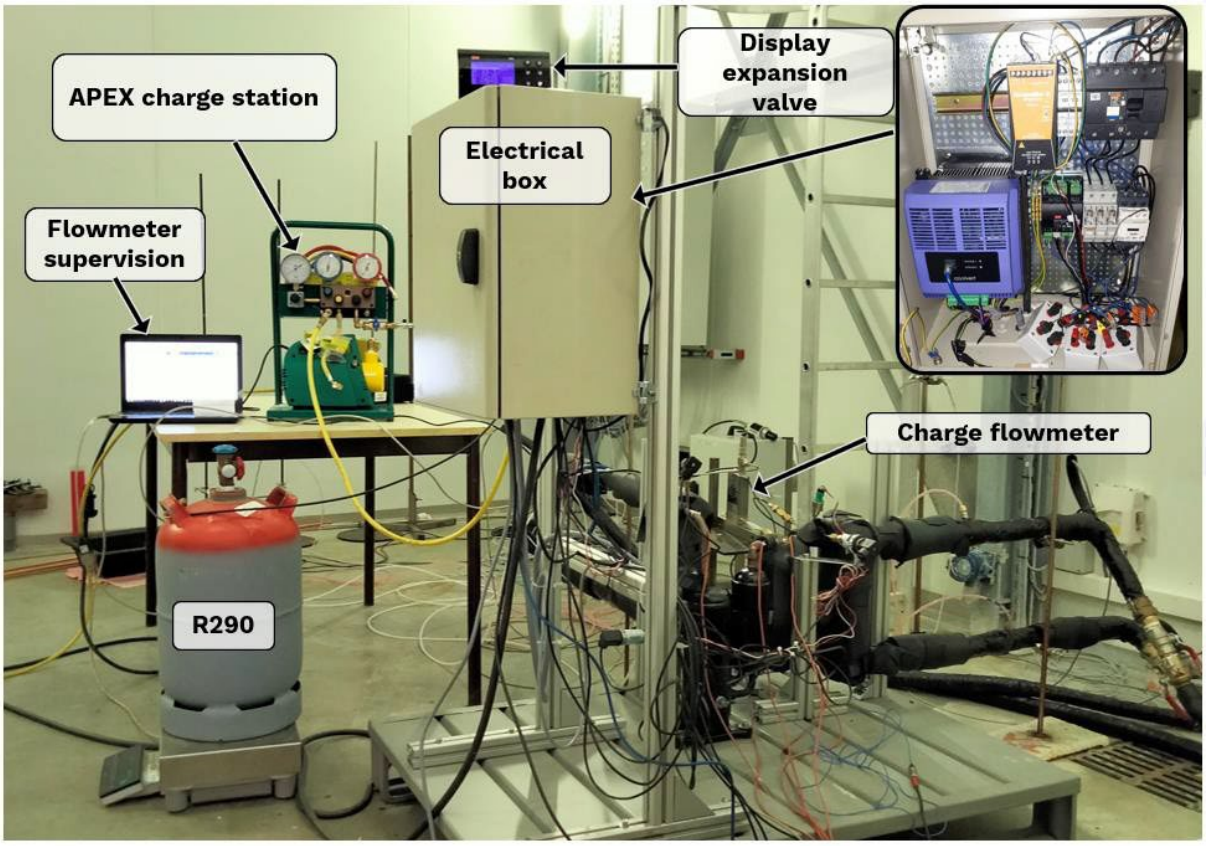

Figure 4-3: Photo of the prototype in the test room

4.1.3 Results and Conclusion

The overall objective of creating a 5-kW unit operating with less than 150 g of propane was achieved (Table 4).

Table 4: Results overview

	Overview of the charge optimization results
Conf. 1	Good operation + optimal charge around **200 g**
Conf 2.	Bad operation + optimal charge around **210 g**
Conf 3.	Good operation + optimal charge around **190 g**
Conf 4.	Good operation + optimal charge around **90 g**
Conf 5.	Good operation + optimal charge around **110 g**

4.1.3.1 Impact of superheating at the compressor inlet

The superheating entering the compressor during refrigerant charge optimization had an influence on the final optimal charge. Increasing superheating decreases optimal charge and degrades performance (Figure 4-4). Reducing the superheating below 10 K does not significantly improve the performance.

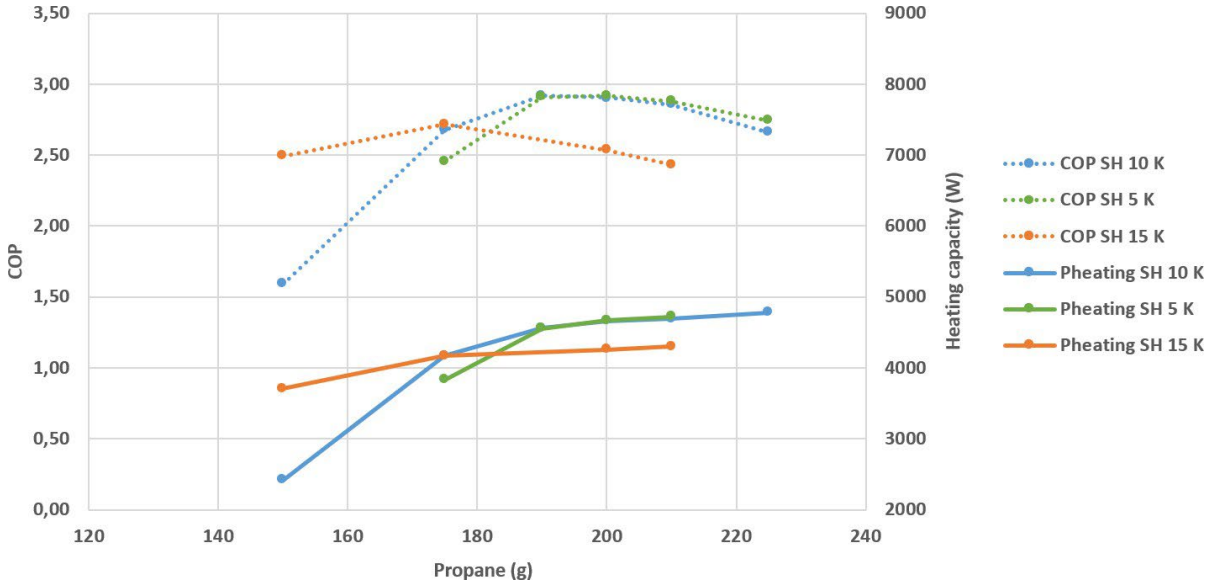

Figure 4-4: Charge optimization – Rotary compressor 60 Hz – Condenser 20 p – Evaporator 30 p EVAP 4 °C / -1 °C – COND 47 °C / 55 °C

4.1.3.2 Impact of compressor speed

The compressor speed does not seem to have any influence on the optimal charge with the low charges encountered (Figure 4-5).

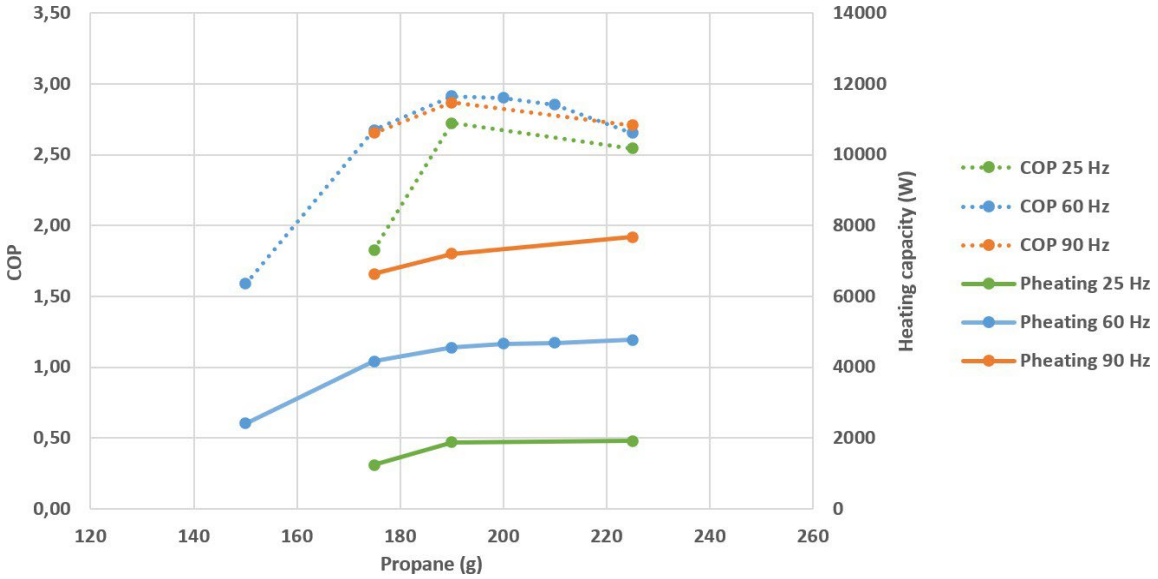

Figure 4-5: Charge optimization – Rotary compressor – Condenser 20 p – Evaporator 30 p – Superheating 10 K EVAP 4 °C / -1 °C – COND 47 °C / 55 °C

4.1.3.3 Impact of evaporator size

Reducing the size of the evaporator makes it possible to reduce the refrigerant load significantly (Figure 4-6). However, the smallest evaporator (20 plates) slightly reduces the performance and the heating capacity of the unit.

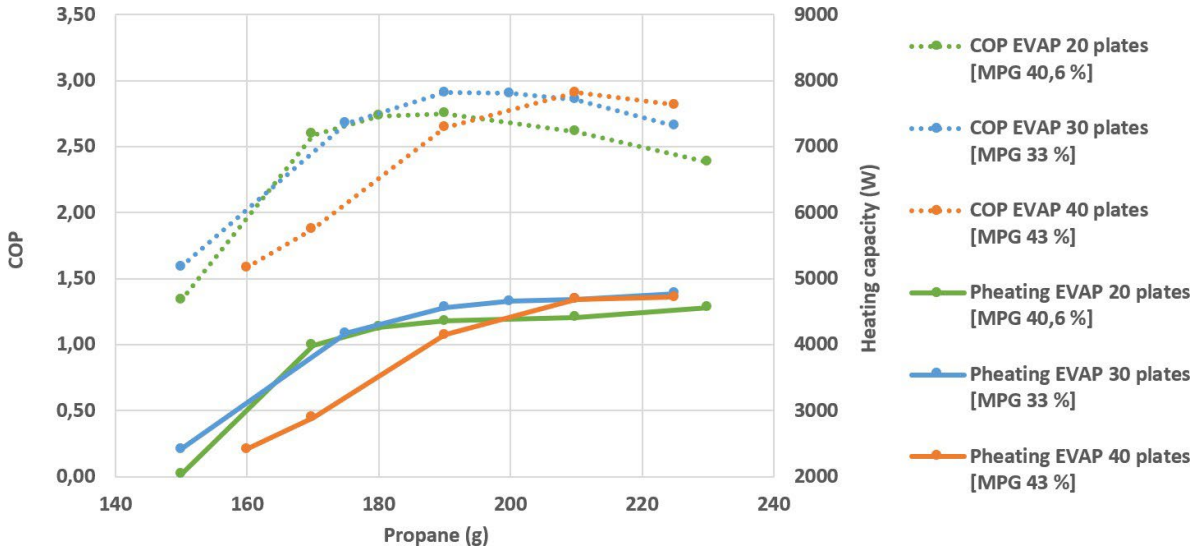

Figure 4-6: Charge optimization – Rotary compressor 60 Hz – Condenser 20 p – Superheating 10 K EVAP 4 °C/ -1 °C (or 3 °C/ 0 °C) – COND 47 °C / 55 °C

It must be noticed that with the largest evaporator (40 plates), the unit could not operate properly with brine temperatures 4 °C / -1 °C because of very low evaporation temperatures. This can be related to the combined effects of the low brine speed between the plates (compared to the smaller heat exchangers) and the high fraction of MPG in the brine mixture. That is why the measurements were made using brine temperature 3 °C / 0 °C with the 40 plates evaporator.

4.1.3.4 Impact of condenser size

Apart from the liquid receivers, condensers are known to be the components with the largest refrigerant charge storage in units. Thus, increasing the condenser size significantly increases the optimal refrigerant charge, even for very low-charge systems (Figure 4-7). In addition, increasing the condenser size also widens the optimal charge range, which can help to better manage the variations in temperature conditions without a liquid receiver.

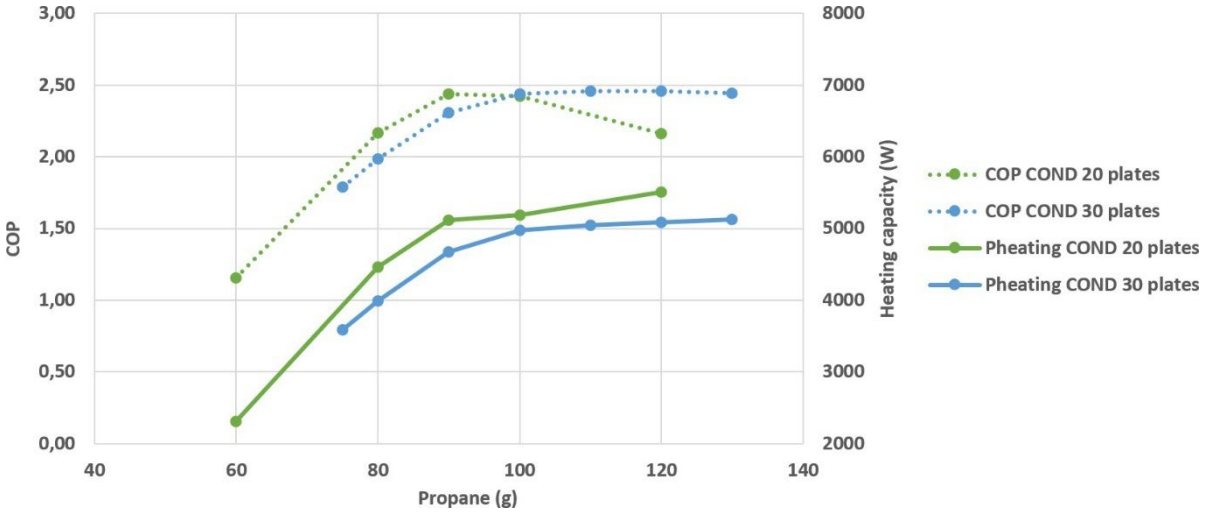

Figure 4-7: Charge optimization – Scroll Compressor 60 Hz – Evaporator 20 p – Superheating 10 K EVAP 4 °C/-1 °C – COND 47 °C/55 °C

4.1.3.5 Impact of compressor type / oil quantity in the system

The use of a semi-hermetic automotive compressor with a small quantity of oil made it possible to reduce the propane charge (Figure 4-8) significantly. This type of compressor, however, presents disappointing performances at low rotation speeds, as observed during seasonal performance analysis.

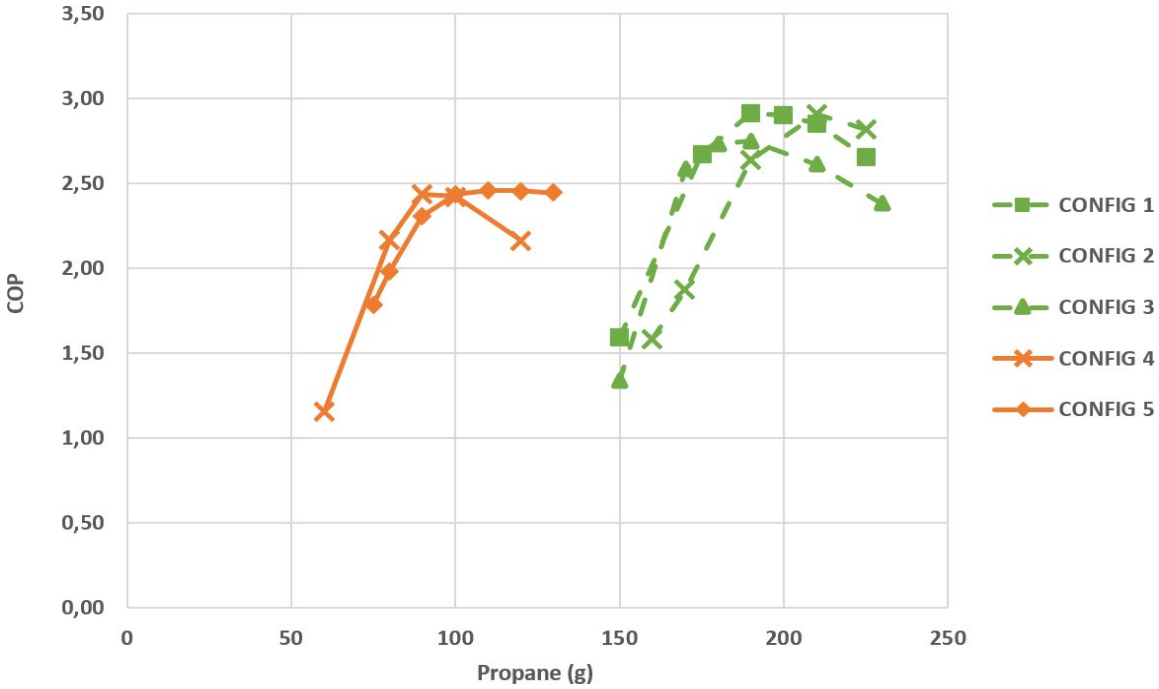

Figure 4-8: Charge optimization – Compressor 60 Hz – Superheating 10 K EVAP 4 °C/-1 °C – COND 47 °C/55 °C (Rotary = Green – Scroll = Orange)

The difference of heating capacity between the two compressors observed when operated at the same rotation speed is proportional to the compressor displacements difference. This difference

being low (30.6 cc versus 33 cc), no link with the refrigerant charge difference can be established. The global internal volume is not known for the scroll compressor even if it can be assumed that the scroll compressor is smaller than the rotary compressor. This difference cannot explain the large difference between both optimal charges. On the contrary, the oil amount seems to be a major difference between the two compressors.

Then reducing the quantity of oil or using a compressor with a low oil requirement are the best option to reduce the refrigerant load below 150 g of propane.

4.1.3.6 Seasonal performances analysis

Configurations 3 and 4 were tested according to conditions adapted from EN 14825 (see Table 4-2) with the optimal charges found during charge optimization: 190 g for configuration 3 and 90 g for configuration 4. For both configurations, the design capacity is 5 kW with a temperature of bivalence of -10 °C.

For conditions E/F, A and B the rotation speed differences are proportional to the compressor displacements difference (Figure 4-9).

Minimum speed compressor was reach for conditions C and D with the rotary compressor, and only for condition D for the scroll compressor (Figure 4-9). Then temperature modifications were applied on these conditions.

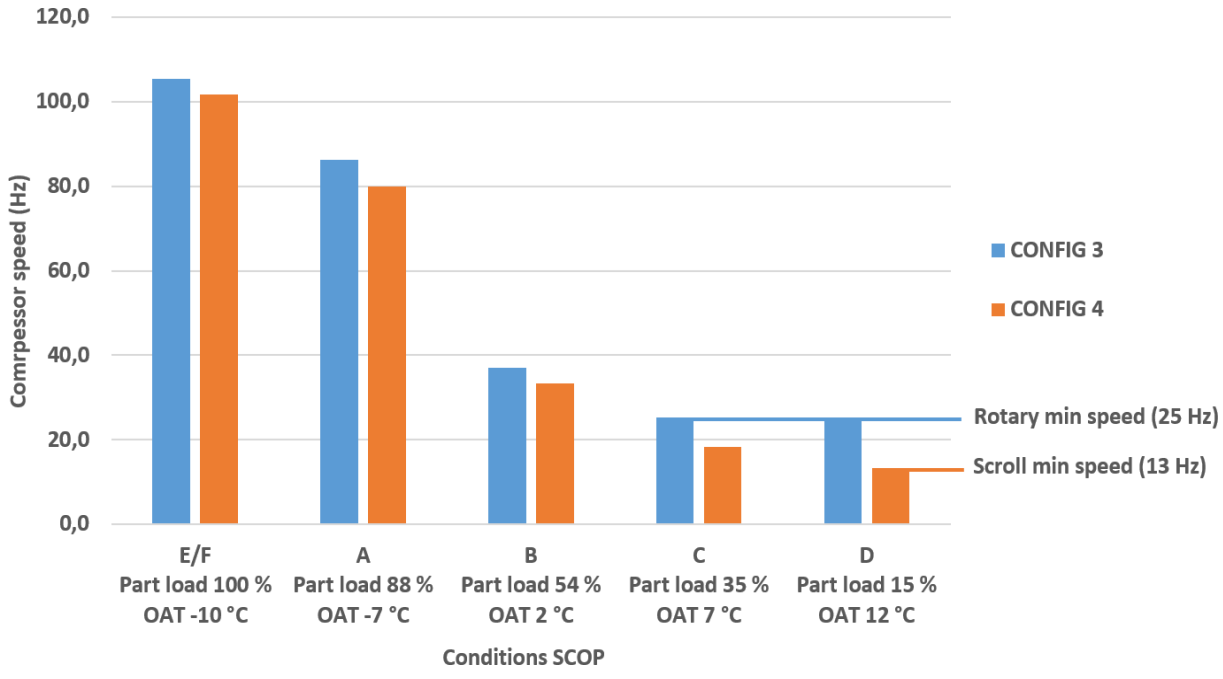

Figure 4-9: Compressor speed for each SCOP conditions

Figure 4-10 shows the condensing and evaporating temperatures for both configurations 3 and 4 in addition to the heat transfer fluid mean temperatures in the two heat exchangers. The evaporating temperatures are the same for the two configurations, whereas the condensing temperatures are higher with configuration 3. This observation can be linked with the analysis of Figure 11.

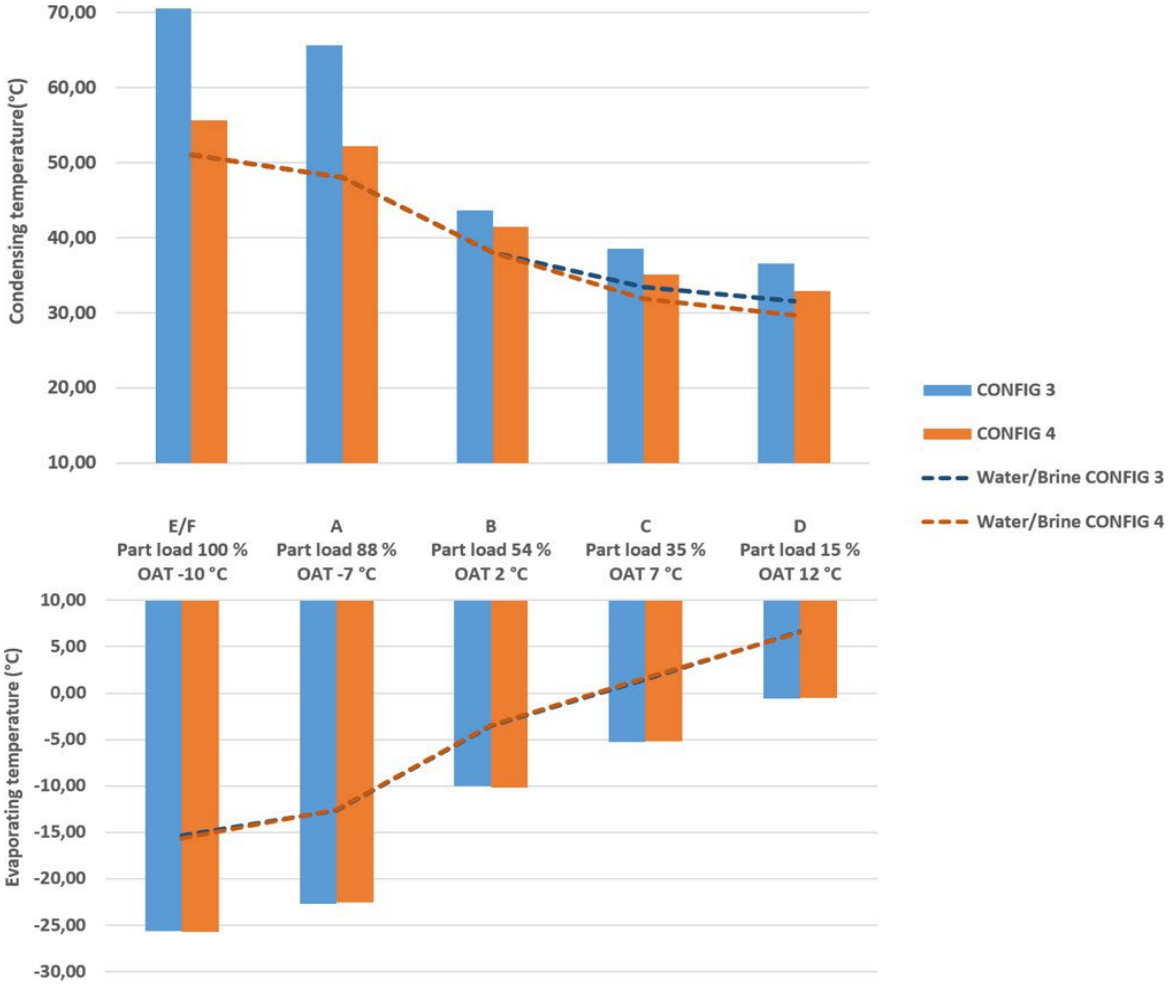

Figure 4-10: Condenser and evaporator temperatures

As depicted in Figure 4-11, the experiments show that when the prototype in configuration 4 operates with a very low refrigerant charge of 90 g, a liquid receiver to manage the conditions variations is unnecessary. Indeed, the subcooling varies from 11 K for conditions E/F to 7 K for conditions D. For configuration 3, however, with 190 g of propane, the subcooling varies between

25 K for conditions E/F to 9 K for conditions D. The unit seems then to be overcharged and a liquid receiver would be needed.

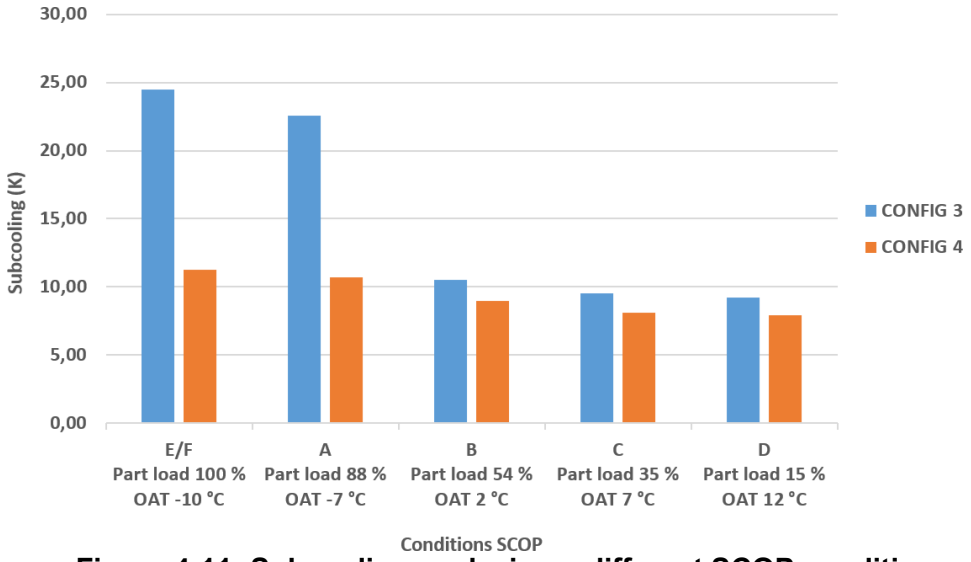

Figure 4-11: Subcooling analysis on different SCOP conditions

The configuration 3 with a rotary compressor and 190 g of propane seems to have two main disadvantages when considering a seasonal performance test compared to configuration 4 with scroll automotive compressor and 90 g of propane:

- higher condensation temperatures due to overcharging for conditions E/F and A
- higher minimum compressor speed causing ON/OFF cycling for conditions C and D

However, as shown in Figure 12, configuration 3 performs better for every condition tested. The lower the heating capacity required, the higher the performance difference is. It appears that the performance of the compressor used in configuration 4 does not improve when its rotation speed and compression ratio decrease.

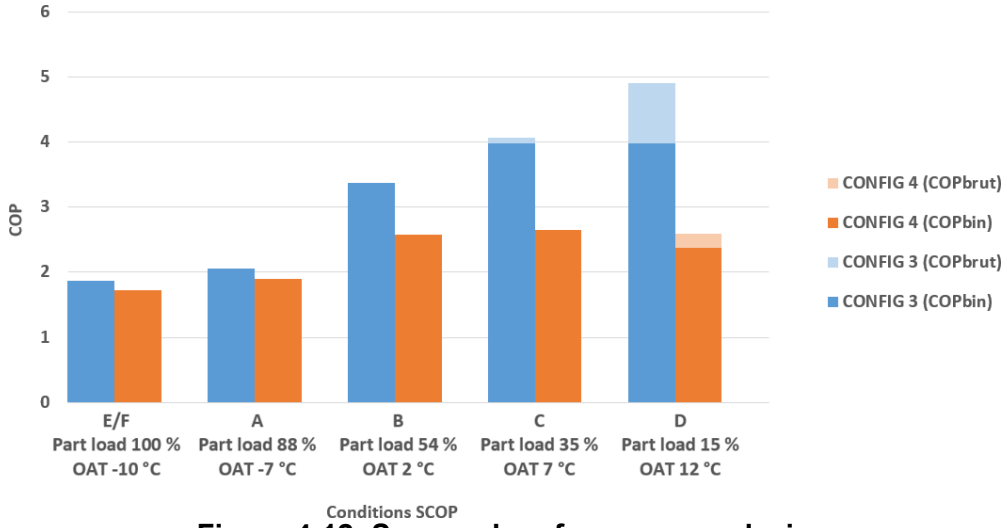

Figure 4-12: Seasonal performance analysis

4.2 Experimental evaluation of R410A, R407C and R134a alternative refrigerants in residential heat pumps

Prepared by:

Pierre PARDO[1]*

[1]CETIAT, Centre Technique des Industries Aérauliques et Thermiques, HVAC systems department, Villeurbanne, France

***Corresponding author e-mail: pierre.pardo@cetiat.fr**

4.2.1 Summary

Alternative refrigerants with low GWP are under investigation for residential heat pumps, air-conditioners, and heat pump water heaters since R410A, R407C, and R134a have GWP of 2088, 1650, and 1430, respectively. In this study, five alternative refrigerants: R459A, R454B, R447A, HPR2A, and R32 were investigated for the replacement of R410A in a 10 kW Air-to-Water (A/W) reversible heat pump. Three alternative refrigerants for R134a: R1234yf, R513A and R450A were tested in a split Heat Pump Water Heater (HPWH) having a water tank of 200 liters. R454C and R455A were evaluated as a possible alternative to R407C in a 3 kW Water-to-Air (W/A) reversible heat pump. A total of 10 alternative refrigerants with low-GWP were evaluated with not less than 130 performance tests. These experimental results will be useful for the HVAC community for facilitating the selection of the most promising candidates for replacement of R410A, R134a and R407C in residential heat pumps.

4.2.2 Introduction

Protocols and regulations such as the Montreal Protocol (1987), the Kyoto Protocol (1997), the European F-gas regulation (2006 revised 2014) cause a shift toward refrigerants with both zero Ozone Depletion Potential (ODP) and low Global Warming Potential (GWP) [01]. These new limitations lead to the progressive phase-out of HFC and to their replacement by the 4th generation of refrigerants based on HFO mixtures.

Alternative refrigerants with low-GWP are under investigation for residential heat pumps, air-conditioners and heat pump water heaters, since R410A, R407C and R134a have GWP of 2088, 1650 and 1430, respectively. These investigations are numerical ([1], [2]) or experimental ([3], [4], [5], [6]).

The objective of this work is to assess and to compare the heat pump performance when drop-in tests are carried with:

- 5 alternative refrigerants to R410A in a 10 kW air-to-water reversible heat pump: R459A, R454B, R447A, HPR2A and R32, with GWP of 460, 466, 583, 600 and 675, respectively;
- 2 alternative refrigerants to R407C in a 3 kW water-to-air reversible heat pump: R454C and R455A with a GWP of 148 and 146;

- 3 alternative refrigerants to R134a in a split Heat Pump Water Heater (HPWH) having a water tank of 200 liters: R1234yf, R513A, R450A with GWP of 4, 631 and 604, respectively.

The choice of the alternative refrigerants is based on the result analysis of the AHRI Low-GWP AREP Program ([3], [4], [7]).

This work is divided in three parts:

- experimental evaluation of R410A alternative refrigerants in an air-to-water reversible heat pump;
- experimental evaluation of R407C alternative refrigerant in a water-to-air reversible heat pump;
- experimental evaluation of R134a alternative refrigerants in a split water heater heat pump.

For each part, the refrigerant properties are presented, then the experimental procedure is described, and finally the experimental results are reported and analyzed.

In this study, only performance tests were carried out, the use of these alternative refrigerants will require a complete study of the risks, sizing and compatibility.

4.2.3 Experimental evaluation of R410A alternative refrigerants in an Air-to-water reversible heat pump

4.2.3.1 Properties of alternative refrigerants to R410A

Table 4-2 presents the main properties of the refrigerants studied to replace R410A. The data source is the software NIST REFPROP Version 10 [8]. Figure 4-13 shows the refrigerant's GWP and safety class.

Table 4-2: Refrigerant properties

Refrigerant	Composition	GWP_{100}	Critical temperature (°C)	Normal boiling point (°C)	Glide (K)	Safety class
R410A	R32/R125 (50/50 wt.%)	2088	70.2	-51.6	0.1	A1
R32	R32 (100 wt.%)	675	78.0	-52.0	0	A2L
HPR2A	R32/R134a/R1234ze (76/6/18 wt.%)	600	82.0	-50.7	4.1	A2L
R447A	R32/R1234ze(E)/R125 (68/28.5/3.5 wt.%)	583	80.2	-47.6	5.1	A2L
R454B	R32/R1234yf (68.9/31.1 wt.%)	466	78.1	-50.4	1.3	A2L
R459A	R32/R1234yf/R1234ze (68/26/6 wt.%)	460	76.5	-49.5	1.9	A2L

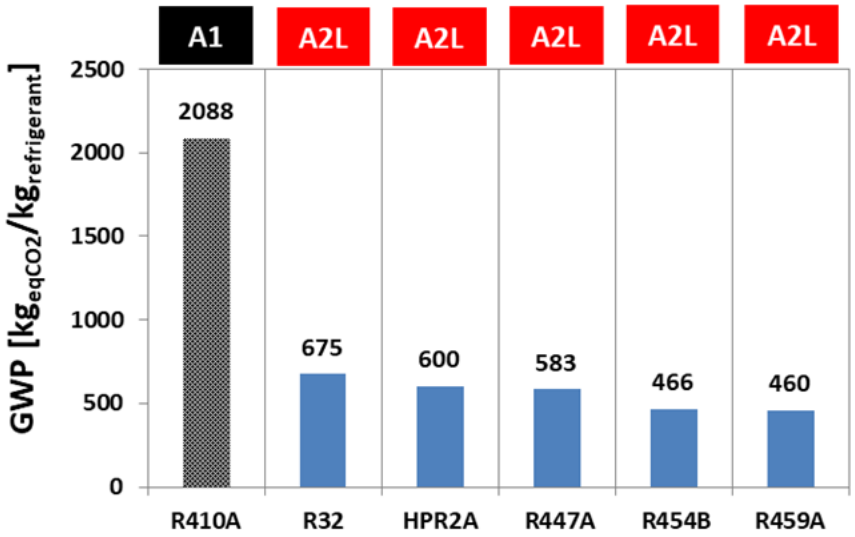

Figure 4-13: Refrigerant's GWP and safety class

Alternative refrigerants have a lower GWP than R410A, between -67 % and -78 %. Except for R32, which is a pure refrigerant, the other alternatives are mixtures and mainly composed of R32 (~70 wt.%) and an HFO (~30 wt.%), R1234ze(E) or R1234yf. The safety class of alternative refrigerants is A2L, which means they have low flammability and are non-toxic. All alternative mixtures have a glide. The saturation properties (pressure-temperature) are shown in Figure 4-14. The five refrigerants have equivalent saturation properties. R447A, R454B, R459A, and HPR2A remain slightly less volatile than R410A and R32.

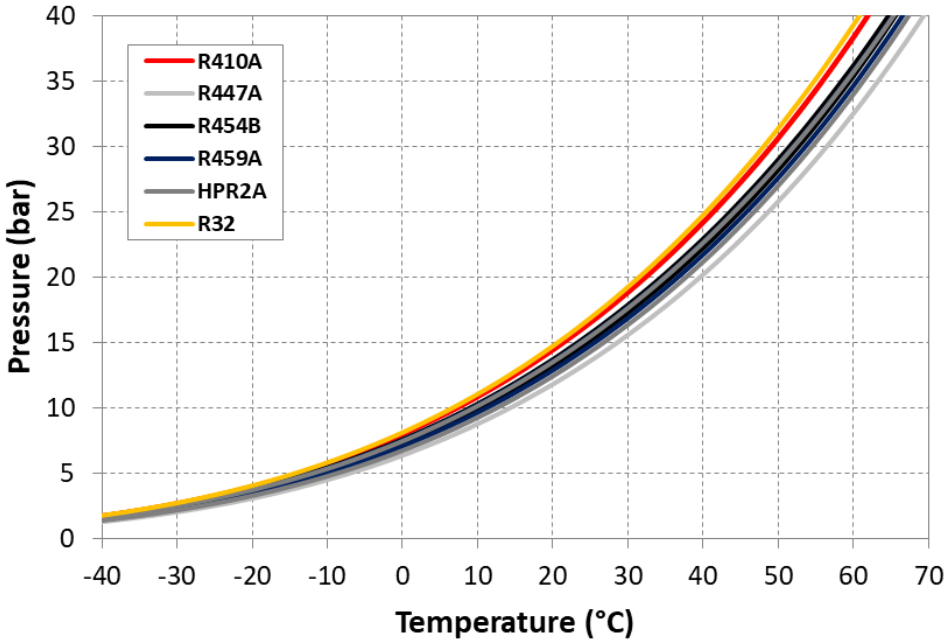

Figure 4-14 : Saturation properties: Pressure-Temperature

4.2.3.2 Experimental investigation

Drop-in tests were carried out to assess the heat pump performance. The heating capacity of the tested air-to-water heat pump is close to 10 kW at H1 rating condition. It is a reversible, packaged, and non-ducted appliance. The heat pump is equipped with a fixed capacity scroll compressor and a calibrated orifice as an expansion device. The initial charge of R410A is 2.35 kg.

The test conditions in cooling mode and in heating mode are described in Table 4-3 and Table 4-4, respectively. For each refrigerant, a charge optimization was done at the C1 rating condition, then the rating and operating limit condition tests were performed, and finally, performance verification with R410A was carried out on C1 and H1 rating conditions to detect any anomaly after the use of the alternatives. The tests were carried out in one of CETIAT climatic rooms according to EN 14511 standard [11]. During tests, measurements allowed the determination of thermal capacities, electric energy consumptions, efficiencies (EER or COP), as well as pressures and temperatures on the refrigerant circuit.

According to the uncertainty of measurement on the laboratory's instrumentation, capacities were determined with a maximal uncertainty of 5 % and electric energy consumptions with a maximal uncertainty of 1 %.

Table 4-3: Rating (C) and operating limit conditions (CL) in cooling mode

	Air temperature (°C)	Inlet water temperature (°C)	Outlet water temperature (°C)
C1	35	12	7
C2	35	23	18
CL1	18	*	5
CL2	42	*	25

* Inlet water temperature obtained with the C1 water flow rate.

Table 4-4: Rating (H) and operating limit conditions (HL) in heating mode

	Dry air temperature (wet bulb) (°C)	Inlet water temperature (°C)	Outlet water temperature (°C)
H1	7(6)	30	35
H2	7(6)	40	45
H3	7(6)	47	55
H4	-7(-8)	*	35
H5	2(1)	*	35
H6	12(11)	*	35
HL1	-15	*	22
HL2	-10	*	42.5
HL3	24 (20)	*	54.8

* Inlet water temperature obtained with the H1 water flow rate.

The operating limit conditions were fixed by the heat pump manufacturer: they correspond to the boundary conditions of operation of the heat pump with R410A. During the test, the discharge temperature was limited to 115 °C to avoid any damage to the compressor.

4.2.3.3 Results of the experimental evaluation of R410A alternative refrigerants

4.2.3.3.1 Charge optimization

The initial alternative refrigerant charge was about 1.65 kg (corresponding to 70 % of the initial R410A charge) to perform the charge optimization. At C1 rating condition (see Table 4-3), refrigerant was added (+50 g every 30 minutes) while four parameters were monitored: EER, cooling capacity, superheating, and subcooling. The objective was to identify the performance curve inflection point to determine the optimal charge. Particular attention was paid to the fact that superheating and subcooling have to be comprised between 4 and 7 K. The optimal charges obtained are reported in Table 4-5.

Table 4-5: Charge optimization results (at C1 rating condition)

Refrigerant	R410A (baseline)	R32	R454B	R459A	HPR2A	R447A
Charge (kg)	2.35	1.52 *(-35.1 %)*	2.00 *(-14.9 %)*	1.96 *(-16.5 %)*	1.80 *(-23.4 %)*	1.86 *(-20.8 %)*
Cooling capacity (kW)	8.01	8.63 *(+7.7 %)*	8.25 *(+3.0 %)*	7.93 *(-1.0 %)*	7.75 *(-3.2 %)*	7.44 *(-7.1 %)*
EER (-)	2.71	2.83 *(+4.4 %)*	2.97 *(+9.6 %)*	2.90 *(+7.1 %)*	2.90 *(+7.0 %)*	2.83 *(+4.4 %)*
Superheating (K)	9.40	8.10 *(-1.3 K)*	4.10 *(-5.3 K)*	4.30 *(-5.1 K)*	4.30 *(-5.1 K)*	4.10 *(-5.3 K)*
Subcooling (K)	6.10	1.20 *(-4.9 K)*	4.50 *(-1.5 K)*	5.60 *(-0.5 K)*	2.00 *(-4.1 K)*	3.70 *(-2.4 K)*

Alternative refrigerant charges are lower (-35 % to -15 %) than with R410A. These results are consistent with the literature ([3], [5], [9], [10]).

4.2.3.3.2 Cooling mode

Figure 4-15 presents the results obtained in cooling mode: ratios of performance (alternative/R410A) and discharge temperature. Table 4-6 and Table 4-7 provide values for the heat pump cooling capacity and EER, respectively.

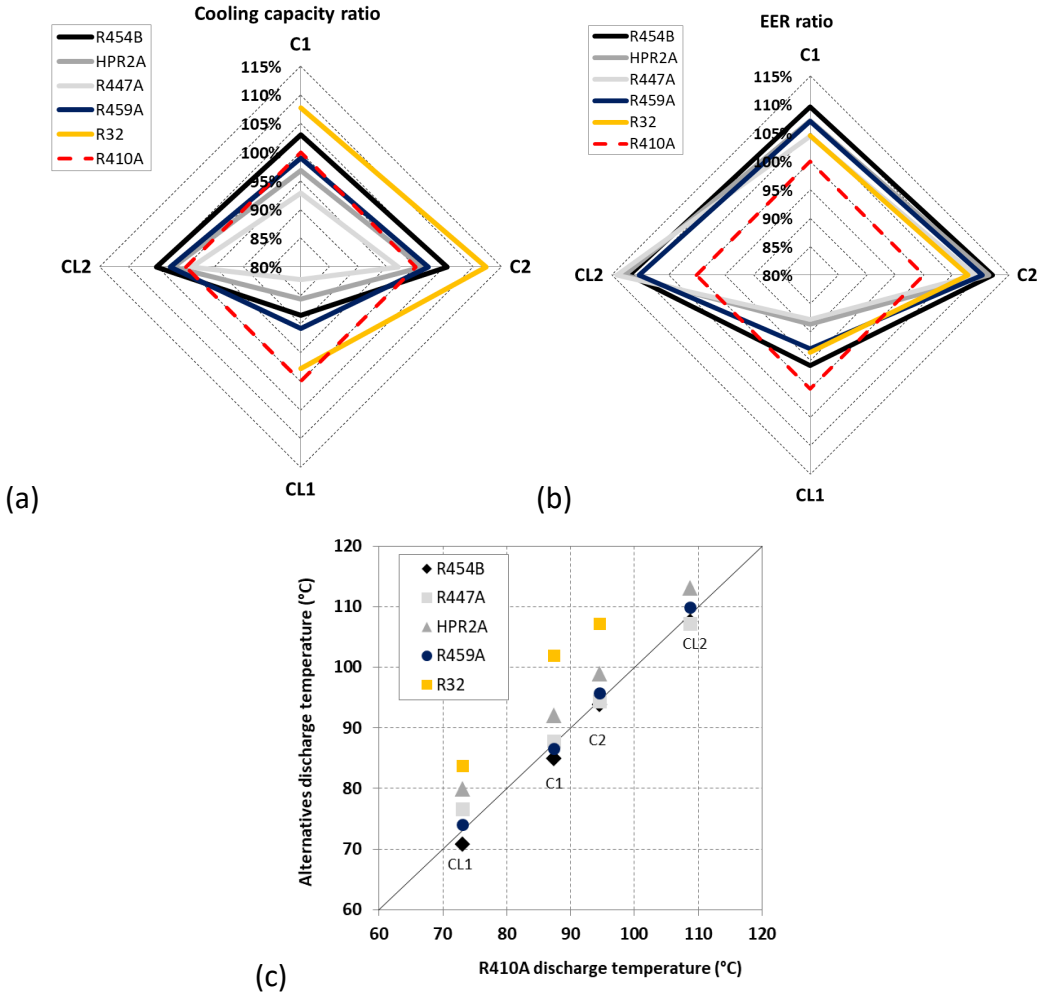

Figure 4-15: Heat pump performance in cooling mode: (a) Capacity ratio; (b) EER ratio; (c) Discharge temperature

Table 4-6: Cooling capacity (green color highlights best performance)

Cooling capacity (kW) Ratio (alternative/base)	R410A (base)	R32	R454B	R459A	HPR2A	R447A
C1 (A35/W12-7)	8.01	**8.63** ***(107.7 %)***	8.25 *(103.0 %)*	7.93 *(99.0 %)*	7.75 *(96.7 %)*	7.44 *(92.9 %)*
C2 (A35/W23-18)	8.80	**9.88** ***(112.3 %)***	9.29 *(105.5 %)*	9.00 *(102.3 %)*	8.90 *(101.1 %)*	8.54 *(97.0 %)*
CL1 (A18/W*-5)	**9.30**	9.09 *(97.8 %)*	8.22 *(88.4 %)*	8.44 *(90.7 %)*	7.97 *(85.7 %)*	7.65 *(82.3 %)*
CL2 (A42/W*-25)	8.87	**Discharge T > 115 °C**	**9.32** ***(105.1 %)***	9.11 *(102.7 %)*	9.06 *(102.1 %)*	8.78 *(99.0 %)*

Table 4-7: EER (green color highlights best performance)

EER (-) Ratio (alternative/base)	R410A (base)	R32	R454B	R459A	HPR2A	R447A
C1 (A35/W12-7)	2.71	2.83 *(104.5 %)*	**2.97 *(109.6 %)***	2.90 *(107.1 %)*	2.90 *(107.2 %)*	2.83 *(104.4 %)*
C2 (A35/W23-18)	2.93	3.16 *(107.8 %)*	**3.29 *(112.1 %)***	3.24 *(110.3 %)*	3.27 *(111.5 %)*	3.20 *(109.1 %)*
CL1 (A18/W*-5)	**3.78**	3.54 *(93.6 %)*	3.62 *(95.9 %)*	3.51 *(93.0 %)*	3.35 *(88.7 %)*	3.32 *(87.8 %)*
CL2 (A42/W*-25)	2.53	**Discharge T > 115°C**	2.83 *(111.9 %)*	2.79 *(110.1 %)*	2.85 *(112.7 %)*	**2.89 *(114.1 %)***

With the exception of the CL1 limit condition, the alternative refrigerants show higher performance than R410A. The cooling capacities at C1, C2, and CL2 conditions are increased with R454B (+3 % to +5.5 %), equivalent or even higher with R459A (-1 % to +2.7 %), equivalent and lower with HPR2A (-3.3 % to +2.1 %) and lower with R447A (-7.1 % to -1 %). R32 leads to higher capacities (+7.7 % to +12.3 %) than R410A at C1 and C2 conditions.

All refrigerants show cooling capacities lower than those with R410A at CL1 limit condition, from -17.7 % with R447A to -2.2 % with R32. EER is better with alternative refrigerants at conditions C1, C2, and CL2 (+4.4 % to + 14.1 %). For CL1 limit condition, all refrigerants give lower EER (-12.2 % to -4.1 %) than R410A. With the exception of CL1, alternative refrigerants achieve equivalent or even better performance than R410A.

The discharge temperatures observed for alternative refrigerants (except R32) in cooling mode are close to those with R410A. R32 did not allow performing CL2 limit condition test because the discharge temperature was higher than 115 °C. To reach a temperature below 115 °C, the outlet water temperature was set to 14 °C.

4.2.3.3.3 Heating mode

Figure 4-16 presents the results obtained in heating mode: ratios of performance (alternative/R410A) and discharge temperature. Table 4-8 and Table 4-9 show values of the heat pump heating capacity and COP, respectively.

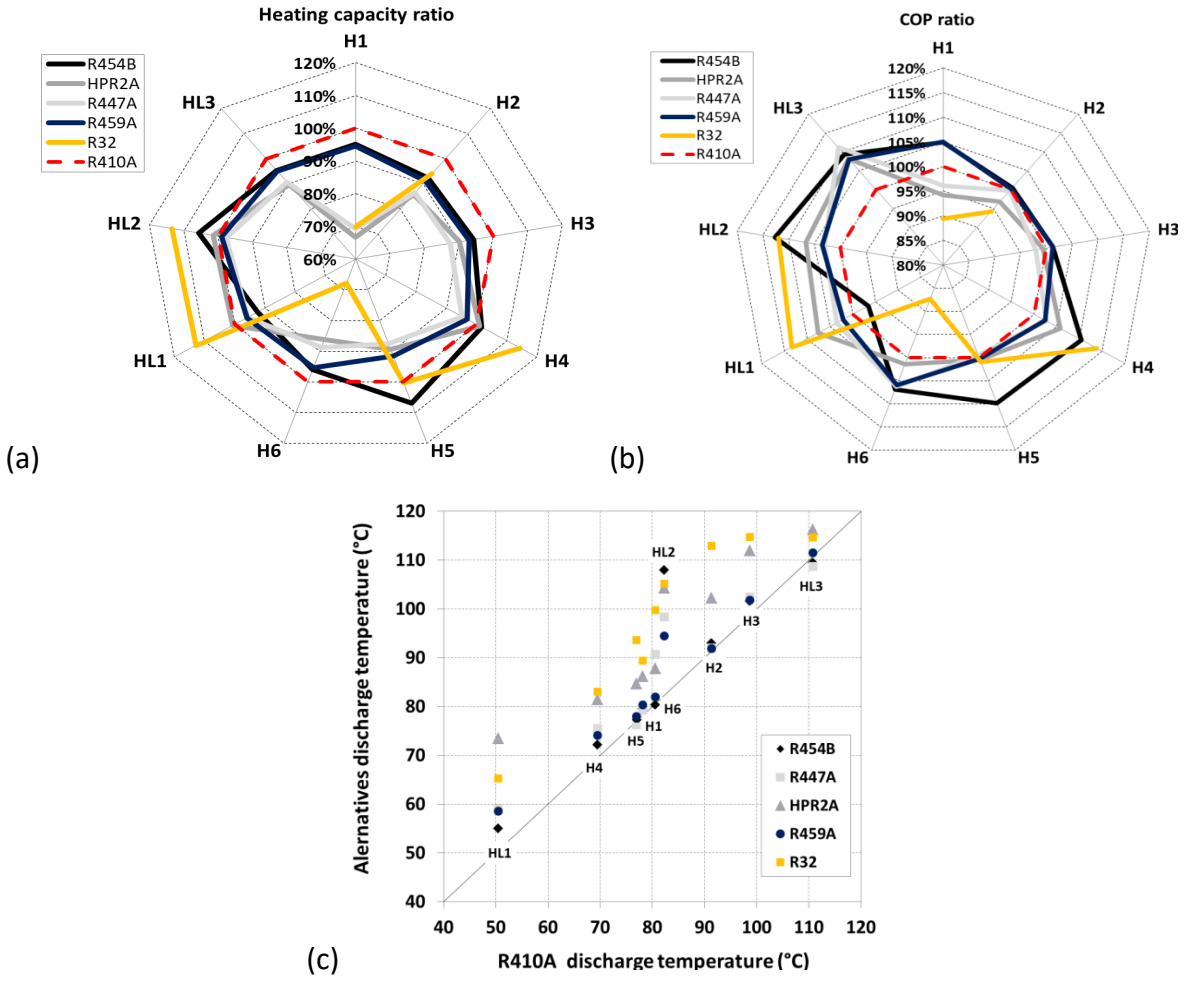

Figure 4-16: Heat pump performance in heating mode: a) Capacity ratio; b) COP ratio; c) Discharge temperature

Table 4-8: Heating capacity (green color highlights best performance)

Heating capacity (kW) (ratio alternative/base)	R410A (base)	R32	R454B	R459A	HPR2A	R447A
H1 (A7(6)/W30-35)	**10.10**	7.06 *(69.9 %)*	9.60 *(95.0 %)*	9.55 *(94.6 %)*	6.73 *(66.6 %)*	6.99 *(69.2 %)*
H2 (A7(6)/W40-45)	**10.44**	9.81 *(94.0 %)*	9.63 *(92.3 %)*	9.51 *(91.1 %)*	8.94 *(85.7 %)*	9.03 *(86.5 %)*
H3 (A7(6)/W47-55)	**9.95**	**Discharge T > 115 °C**	9.38 *(94.3 %)*	9.26 *(93.1 %)*	8.98 *(90.2 %)*	8.71 *(87.6 %)*
H4 (A-7(-8)/W*-35)	4.33	**4.95 *(114.4 %)***	4.40 *(101.7 %)*	4.20 *(97.0 %)*	4.37 *(101.1 %)*	4.12 *(95.3 %)*
H5 (A2(1)/W*-35)	6.21	6.23 *(100.4 %)*	**6.63 *(106.8 %)***	5.68 *(91.6 %)*	5.54 *(89.3 %)*	5.43 *(87.5 %)*
H6 (A12(11)/W*-35)	**10.86**	7.36 *(67.7 %)*	10.43 *(96.0 %)*	10.34 *(95.2 %)*	9.37 *(86.3 %)*	9.64 *(88.7 %)*
HL1 (A-15/W*-22)	3.50	**3.95 *(113.0 %)***	3.23 *(92.5 %)*	3.35 *(95.9 %)*	3.52 *(100.6 %)*	3.34 *(95.6 %)*
HL2 (A-10/W*-42,5)	3.71	**4.21 *(113.6 %)***	3.91 *(105.6 %)*	3.67 *(99.1 %)*	3.76 *(101.5 %)*	3.62 *(97.6 %)*
HL3 (A24(20)/W*-54,8)	**12.33**	**Discharge T > 115 °C**	11.75 *(95.3 %)*	11.71 *(95.0 %)*	11.06 *(89.7 %)*	11.18 *(90.7 %)*

Table 4-9: COP (green color highlights best performance)

COP (-) (ratio alternative/base)	R410A (base)	R32	R454B	R459A	HPR2A	R447A
H1 (A7(6)/W30-35)	3.88	3.47 *(89.6 %)*	4.07 *(104.9 %)*	**4.07 *(105.1 %)***	3.65 *(94.2 %)*	3.73 *(96.2 %)*
H2 (A7(6)/W40-45)	3.30	3.11 *(94.3 %)*	**3.31 *(100.5 %)***	3.30 *(100.2 %)*	3.19 *(96.8 %)*	3.28 *(99.7 %)*
H3 (A7(6)/W47-55)	2.67	**Discharge T > 115 °C**	**2.70 *(101.3 %)***	2.70 *(101.2 %)*	2.65 *(99.3 %)*	2.61 *(97.9 %)*
H4 (A-7(-8)/W*-35)	2.11	**2.40 *(113.9 %)***	2.33 *(110.5 %)*	2.16 *(102.5 %)*	2.23 *(105.8 %)*	2.16 *(102.7 %)*
H5 (A2(1)/W*-35)	3.03	3.06 *(101.1 %)*	**3.32 *(109.8 %)***	3.03 *(100.2 %)*	3.04 *(100.5 %)*	3.01 *(99.5 %)*
H6 (A12(11)/W*-35)	4.10	3.58 *(87.3 %)*	**4.38 *(106.8 %)***	4.34 *(105.9 %)*	4.16 *(101.4 %)*	4.36 *(106.3 %)*
HL1 (A-15/W*-22)	2.16	**2.45 *(113.5 %)***	2.09 *(96.5 %)*	2.21 *(102.1 %)*	2.32 *(107.6 %)*	2.24 *(103.5 %)*
HL2 (A-10/W*-42,5)	1.58	1.77 *(112.2 %)*	**1.78 *(112.7 %)***	1.63 *(103.5 %)*	1.68 *(106.7 %)*	1.63 *(103.1 %)*
HL3 (A24(20)/W*-54,8)	3.05	Discharge T > 115 °C	3.33 *(109.4 %)*	3.29 *(108.0 %)*	3.30 *(108.1 %)*	**3.39 *(111.2 %)***

With the exception of H4, H5, HL1, and HL2 conditions, the alternative refrigerants lead to lower heating capacities than R410A. COPs are equivalent or greater for all the conditions. The heating capacity at H1 rating condition (Figure 4-16 a)) is significantly reduced with R447A, HPR2A, and R32 because the heat pump has carried out defrosting cycles that did not occur during the tests with R454B, R459A, and R410A.

R454B and R459A lead to heating capacities lower or equivalent than R410A, from -7.5 % to +6.8 % and from -8.9 % to -1.1 %, respectively. Heating capacities with HPR2A are lower or equivalent to those with R410A (-33.4 % to +1.3 %). R447A shows lower heating capacities than R410A (-30.8 % to -2.4 %). R459A achieves equal or greater COPs than R410A (+0.2 % to +8 %).

All COPs with R454B are equivalent or greater than with R410A (+0.5 % to +12.7 %), with the exception of the HL1 limit condition where it is lower (-3.5 %), HPR2A obtains COPs equal or greater than R410A (-0.7 % to +8.9 %) for H3 to HL2 conditions and lower for H1 and H2 conditions (-5.8 % and -3.2 %). R447A shows lower or equivalent COPs than R410A for the conditions between H1 and H3 (-3.8 % to -0.3 %) and higher or equivalent for the conditions H4 to HL2 (-0.5 % to +11.2 %). Capacities and COPs obtained with R32 for negative air temperatures are significantly greater than those with R410A, between +0.4 % to +14.4 % and +1.1 % to +13.9 %, respectively. For these conditions (H4, HL1, HL2), R32 show the best performances.

There is an important dispersal of the discharge temperatures, but with the exception of R32, the four alternatives get discharge temperatures close to those of R410A. R32 did not allow performing H3 rating condition and HL3 limit conditions, because the discharge temperature was higher than 115 °C. To reach a discharge temperature below 115 °C, the outlet water temperatures were set to 48 °C for H3 and 43 °C for HL3.

4.2.3.3.4 Performance verification

To ensure that the alternative refrigerants did not damage the heat pump, tests with the initial R410A charge (2.35 kg) were performed after each series of tests with the alternative refrigerants. This verification allowed the determination of the heat pump performance deviation, but it does not give any answer concerning the long-term use of the alternative refrigerants. The performance gaps obtained are quite small (from -1 % to +5 %) and within the measurement uncertainty.

According to the results, we can conclude that there was no notable damage to the heat pump after the use of the refrigerant alternatives.

With the exception of R32, the alternative refrigerants might be considered as alternatives to R410A for both modes and all the conditions tested in this study. R454B and R459A showed the best performances. R32 could be used, but the heat pump operating map should be decreased because of high discharge temperatures, especially when condensation occurs at high temperatures.

4.2.4 Experimental evaluation of R407C alternative refrigerant in a water-to-air reversible heat pump

4.2.4.1 Properties of alternative refrigerant to R407C

Table 4-10 presents the main properties of the refrigerant studied to replace R407C. The data source is the software NIST REFPROP Version 10 [8]. Figure 4-18 shows the refrigerant's GWP and safety class.

Table 4-10: Refrigerant properties

Refrigerant	Composition	GWP_{100}	Critical temperature (°C)	Normal boiling point (°C)	Glide (K, at 40°C)	Safety class
R407C	R32/R125/R134a (23/25/52 wt.%)	1,650	86.1	-40.1	7.0	A1
R454C	R1234yf/R32 (78.5/21.5 wt.%)	148	85.7	-42.4	8.5	A2L
R455A	R1234yf/R32/R744 (75.5/21.5/3 wt.%)	146	85.6	-45.6	9.7	A2L

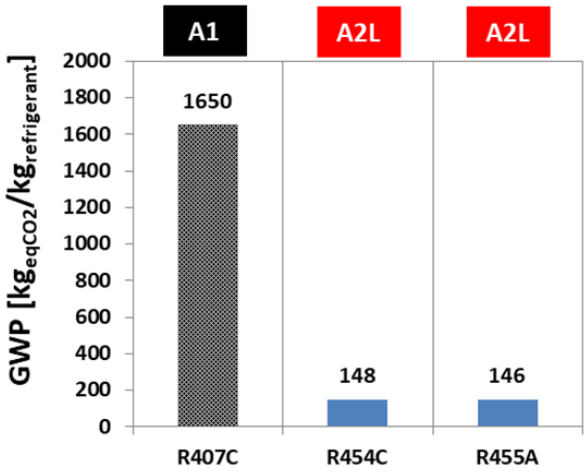

Figure 4-17: Refrigerant's GWP and safety class

The GWP of R454C and R455A are significantly lower than that of R407C (-91 %), and they are below the most compelling GWP limit (150) of the European F-Gas regulation. R454C and R455A have an A2L safety class, which means they have a low flammability and are non-toxic. R454C and R455A have a glide slightly higher than R407C.

The saturation properties (pressure-temperature) are shown in Figure 4-18. The refrigerants have equivalent saturation properties.

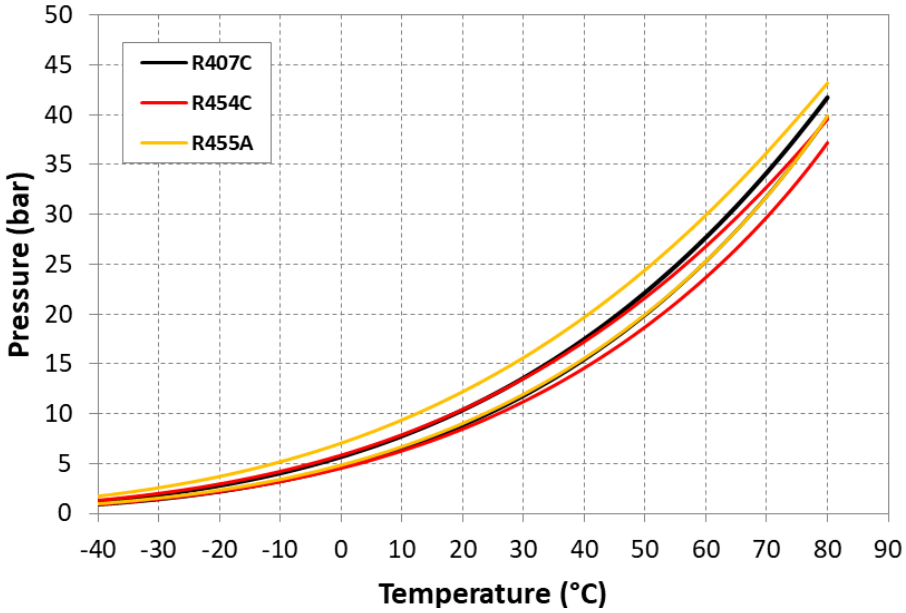

Figure 4-18 : Saturation properties: Pressure-Temperature

4.2.4.2 Experimental investigation

Drop-in tests were carried out to assess the heat pump performance. The heating capacity of the tested water-to-air heat pump is close to 2.9 kW at H1 rating condition (see Table 4-12). It is a reversible, packaged, and ducted appliance. The heat pump is equipped with a fixed-capacity hermetic rotary compressor and a capillary tube as an expansion device. The initial charge of R407C is 0.64 kg.

The test conditions in cooling mode and heating mode are provided in Table 4-11 and Table 4-12, respectively. Charge optimization was done for each refrigerant under the CL2 limit. The rating and operating limit condition tests were performed, and finally, performance verification with R407C was carried out on the C1 rating condition to detect any anomaly. The tests were carried out in one of the CETIAT climatic rooms, according to EN 14511 standard [11]. During tests, measurements allowed the determination of thermal capacities, electric energy consumptions, efficiencies (EER or COP), and pressures and temperatures on the refrigerant circuit.

According to the measurement uncertainty on the laboratory's instrumentation, capacities were determined with a maximal uncertainty of 5 %, and electric energy consumptions with a maximal uncertainty of 1 %.

Table 4-11: Rating (C) and operating limit conditions (CL) in cooling mode

	Inlet water temperature (°C)	Outlet water temperature (°C)	Water flow rate (l/h)	Air temperature (°C)	Air flow rate (m^3/h) (at 1013 mbar and 20°C)
C1	30	35	-	27(19)	475
C2	22	*	485	22(15)	450
CL1	41	*	250	37(27.7)	500
CL2	42	*	250	22(15)	500

Table 4-12: Rating (H) and operating limit conditions (HL) in heating mode

	Inlet water temperature (°C)	Outlet water temperature (°C)	Water flow rate (l/h)	Air temperature (°C)	Air flow rate (m^3/h) (at 1013 mbar and 20°C)
H1	20	17	-	20(15)	475
H2	12	*	250	12(7.2)	500
HL1	36	*	250	27(19.5)	450
HL2	36	*	485	27(19.5)	450

The operating limit conditions were fixed by the heat pump manufacturer: they correspond to the boundary conditions of operation of the heat pump with R407C.

4.2.4.3 Results of the experimental evaluation of R407C alternative refrigerant

4.2.4.3.1 Charge optimization

To perform the charge optimization, the initial alternative refrigerant charge was about 0.416 kg (corresponding to 65 % of the initial R407C charge). At CL2 limit condition, refrigerant was added (+25 g in every 30 minutes) while four parameters were monitored: EER, cooling capacity, superheating and subcooling. The objective was to determine the optimal charge for a superheating close to 2 K. The optimal charges obtained for both refrigerants are reported in Table 4-13. R454C and R407C lead to the same optimum load of 640 g. The charge of R455A is higher, 710 g (+11 %). With the R454C the cooling capacity is higher than that of the R407C, on the other hand the EER is lower. The R455A has lower performance.

Table 4-13: Charge optimization results (at CL2 limit condition)

Refrigerant	R407C (baseline)	R454C	R455A
Charge (kg)	0.64	0.64 *(0 %)*	0.71 *(+11.0 %)*
Cooling capacity (kW)	1.75	1.89 *(+7.7 %)*	1.68 *(-4.2 %)*
EER (-)	2.46	2.44 *(-0.6 %)*	2.06 *(-15.5 %)*
Superheating (K)	3.20	4.80 *(+1.6 K)*	0.7 *(-2.5 K)*
Subcooling (K)	6.80	13.90 *(+7.1 K)*	12.0 *(+5.2 K)*

4.2.4.3.2 Cooling mode

Figure 4-19 presents the results obtained in cooling mode: ratios of performance (alternative/R407C) and the discharge temperature. Table 4-14 provides values for the heat pump cooling capacity and EER.

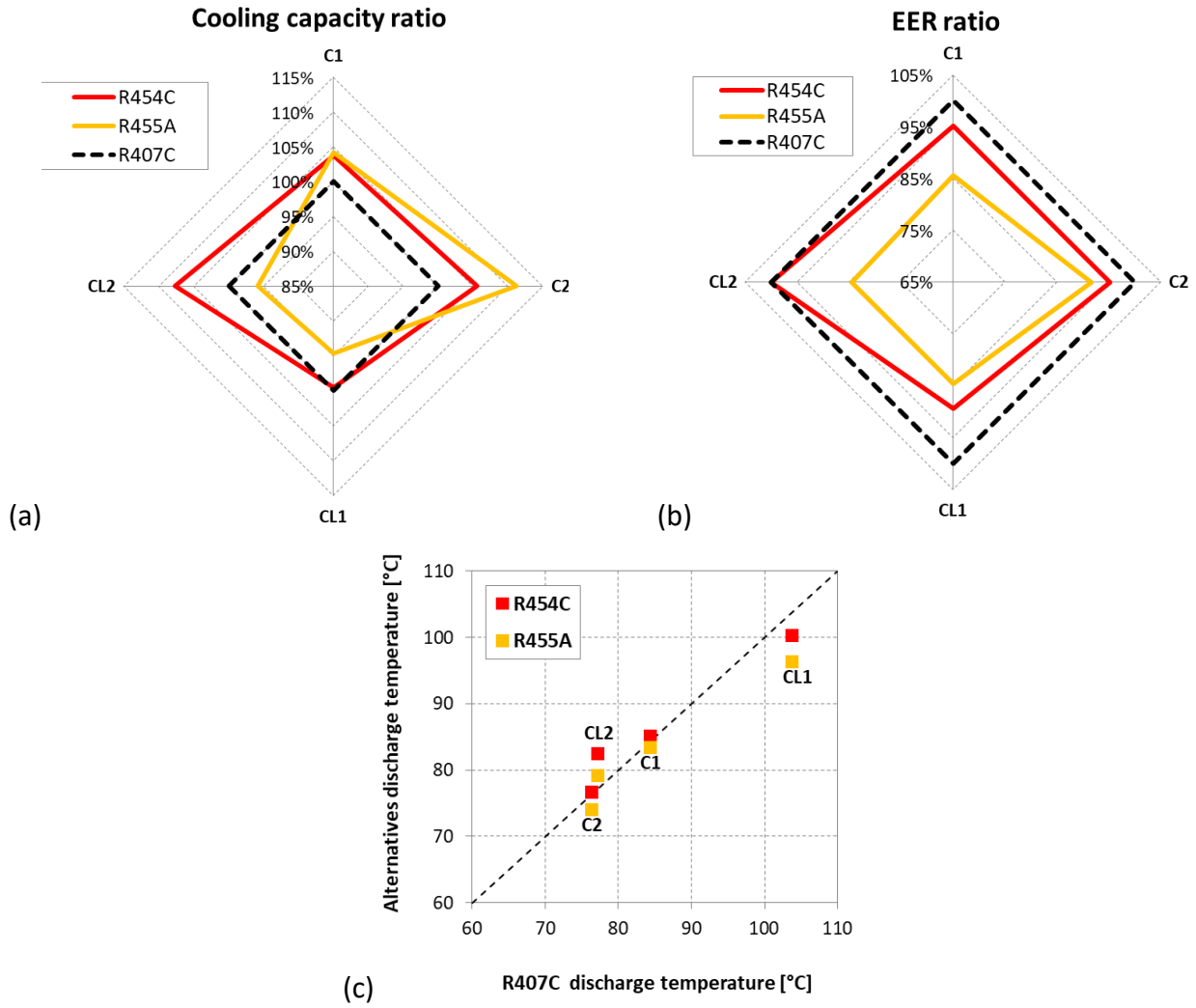

Figure 4-19: Heat pump performance in cooling mode: (a) Capacity ratio, (b) EER ratio; (c) Discharge temperature

Table 4-14: Cooling capacity (green color highlights best performance)

Parameter	**Cooling capacity (kW) (ratio alternative/base)**			**EER (-) (ratio alternative/base)**		
Refrigerant	**R407C (baseline)**	**R454C**	**R455A**	**R407C (baseline)**	**R454C**	**R455A**
C1 (W30-35/A27(19))	2.16	2.24 *(103.7 %)*	**2.24 *(104.1 %)***	**3.70**	3.51 *(95.1 %)*	3.16 *(85.5 %)*
C2 (W22-*/A22(15))	1.97	2.08 *(105.6 %)*	**2.19 *(111.2 %)***	**3.95**	3.76 *(95.2 %)*	3.62 *(91.6 %)*
CL1 (W41-*/A37(27.7))	**2.73**	2.72 *(99.5 %)*	2.58 *(94.6 %)*	**3.36**	3.00 *(89.3 %)*	2.85 *(84.7 %)*
CL2 (W42-*/A22(15))	1.75	**1.89 *(107.7 %)***	1.68 *(95.8 %)*	**2.44**	2.44 *(100.0 %)*	2.06 *(84.5 %)*

The R455A achieves cooling capacities equivalent to or greater than those of R407C (from - 5.4 % to + 11.2 %) but significantly lower EER than those of R407C (from - 15.5 % to - 8.4 %). The R454C achieves higher cooling capacities or equivalent to those of R407C (from -0.5 % to +7.7 %) and lower or equivalent EER (from -10.7 % to 0 %). Under the conditions tested in cooling mode, the R454C shows better performance than the R455A. The discharge temperatures of the three fluids are equivalent.

For R455A, CL1 limit condition was carried out with a water inlet temperature of 36 °C, against 41 °C for the other two, in order to limit the condensing pressure to 30 bar (HP pressure switch limit).

4.2.4.3.3 Heating mode

Figure 4-20 presents the results obtained in heating mode: ratios of performance (alternative/R407C) and discharge temperature. Table 4-15 provides values for heat pump heating capacity and COP.

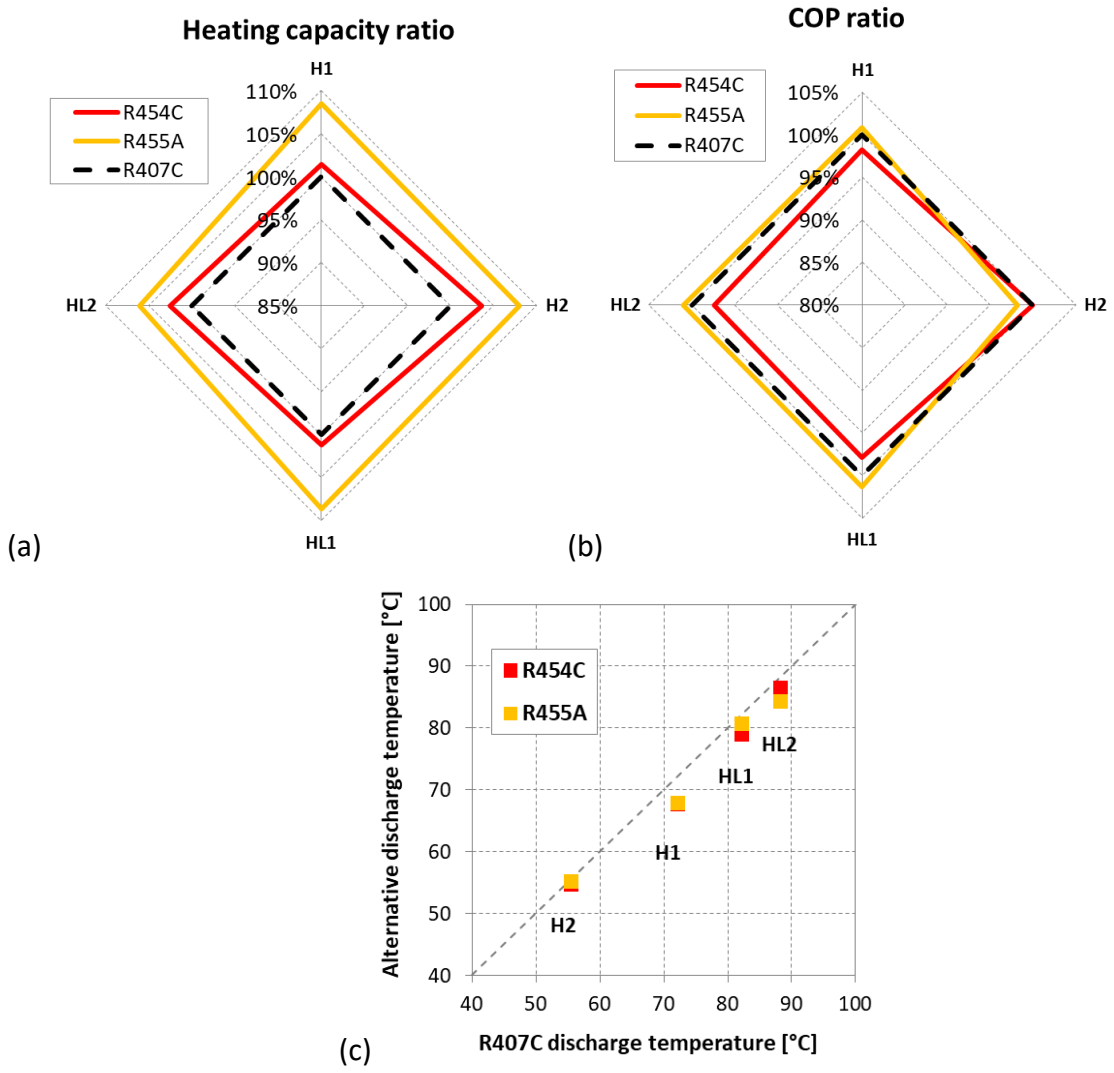

Figure 4-20: Heat pump performance in heating mode: (a) Capacity ratio, (b) EER ratio; (c) Discharge temperature

Table 4-15: Heating capacity (green color highlights best performance)

Parameter	Heating capacity (kW) (ratio alternative/base)			COP (-) (ratio alternative/base)		
Refrigerant	R407C (baseline)	R454C	R455A	R407C (baseline)	R454C	R455A
H1 (W20-17/A20(15))	2.91	2.95 (101.4 %)	3.15 (108.5 %)	4.29	4.22 (98.2 %)	4.33 (100.8 %)
H2 (W12-*/A12(7.2))	2.32	2.41 (103.6 %)	2.51 (108.0 %)	4.37	4.37 (100.0%)	4.30 (98.2 %)
HL1 (W36-*/A27(19.5))	3.23	3.27 (101.2 %)	3.51 (108.6 %)	3.93	3.87 (97.9%)	3.98 (101.3 %)
HL2 (W36-*/A27(19.5))	3.46	3.55 (102.6 %)	3.67 (106.1 %)	4.00	3.97 (97.3%)	4.03 (100.9 %)

R454C obtains higher heating capacities than those of R407C (from + 1 % to + 4 %) and COP equivalent to those of R407C (from -3 % to 0 %). R455A achieves higher heating capacities than those of R407C (from + 6 % to + 8 %) and COP close to those of R407C (from – 2 % to + 1 %). Under the conditions tested in heating mode, R455A performs better than R454C and R407C. The discharge temperatures are equivalent for the three fluids.

4.2.4.3.4 Performance verification

To ensure that R454C and R455A did not damage the heat pump, tests with the initial R407C charge (0.64 kg) were performed. The performance was checked at C1 rating condition. The performance gaps obtained for the cooling capacity and the EER are quite small, +2.5 % and +2.7 %, respectively, and within the measurement uncertainty. According to the results, we can conclude that there was no notable damage to the heat pump after using R454C and R455A.

R454C can be considered as a replacement fluid for R407C without a significant reduction in the performance of the heat pump in its operating range. R455A obtains very good performance in heating mode, while its performance is degraded in cooling mode. In cooling mode, the fluid flows in the finned coil and the plate heat exchanger is co-current. This type of circulation results in a lowering of the evaporating temperature and an increase in the condensing temperature, to the detriment of the EER. With a fluid having a high glide, the performance losses are accentuated.

R454C and R455A have shown encouraging results for the replacement of R407C. The R454C appears to be suitable for replacing the R407C with a reversible machine, since the performance is almost equivalent to that of the R407C in both modes of operation. In heating only mode, with counter-current exchangers, R455A will be the most suitable.

4.2.5 Experimental evaluation of R134a alternative refrigerant in a split heat pump water heater

4.2.5.1 Properties of alternative refrigerants to R134a

Table 4-16 presents the main properties of the refrigerants studied to replace R134a. The data source is the software NIST REFPROP Version 10 [8]. Figure 4-21 shows the refrigerant's GWP and safety class.

Table 4-16: Refrigerant properties

Refrigerant	Composition	GWP_{100}	Critical temperature (°C)	Normal boiling point (°C)	Glide (K)	Safety class
R134a	R134a (100 wt.%)	1,430	101.1	-26.1	0	A1
R513A	R1234yf/R134a (56/44 wt.%)	631	96.5	-29.2	0	A1
R450A	R1234ze(E)/R134a (58/42 wt.%)	604	104.5	-22.6	0.5	A1
R1234yf	R1234yf (100 wt.%)	4	94.7	-29.4	0	A2L

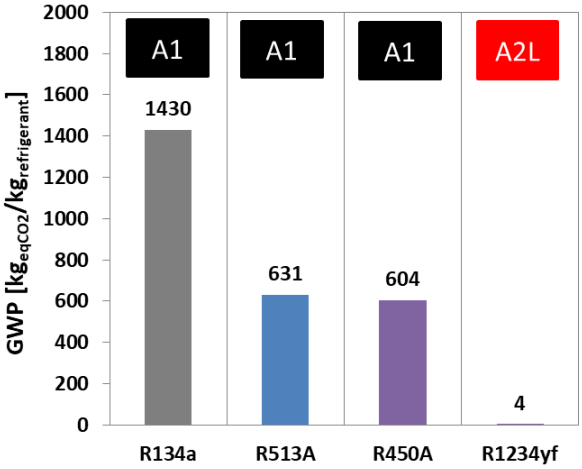

Figure 4-21: Refrigerant's GWP and safety class

The GWP of R513A and R450A are lower than that of R134a. R513A and R450A have an A1 safety class, which means they are non-flammable and non-toxic. R513A has no glide. R450A has a glide of 0.5 K. The GWP of R1234yf is significantly lower than that of R134a, and it is below the most compelling GWP limit (150) of the European F-Gas regulation. R1234yf has an A2L safety class, which means it has a low flammability and is non-toxic. The saturation properties (pressure-temperature) are shown in Figure 4-22. The three refrigerants have equivalent saturation properties. R450A remains slightly less volatile than R134a.

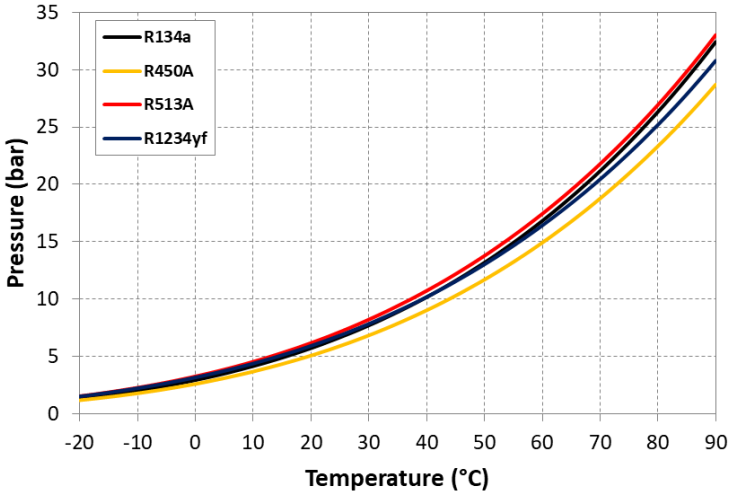

Figure 4-22: Saturation properties: Pressure-Temperature

4.2.5.2 Experimental investigation

Drop-in tests were carried out to assess the performance of the heat pump water heater (HPWH). The HPWH in the test is a split system with a water tank of 200 l. It has a fixed-capacity hermetic rotary compressor and an electronic expansion device. The initial charge of R134a is 1.6 kg. The tests consisted of heating up the water in the tank. When the desired temperature was reached (measured at the top of the tank by a Pt100 sensor), 10 liters/min hot water tapping was performed to determine the energy content until the tapped water reached the initial water temperature. During all tests, measurements allowed the determination of electric power inputs, refrigerant pressures and temperatures, water tank temperature, and energy of the hot water tapping. For each refrigerant, a charge optimization was done, and then heating up of the tank was performed for three outdoor air temperatures. Finally, performance verification with R134a was carried out to detect any anomaly. Refrigerants are compared based on the heating up time, the COP (= water energy content/ electric energy consumption), and the maximal discharge temperature. The tests were carried out in one of the CETIAT climatic rooms. According to the measurement uncertainty on the laboratory's instrumentation, capacities were determined with a maximal uncertainty of 5 %, and electric energy consumptions with a maximal uncertainty of 1 %. The test conditions in charge optimization and performance evaluation are described in Table 4-17 and Table 4-18, respectively.

Table 4-17: Test conditions for charge optimization

Phase 1: Heating up				Phase 2: Water tapping		
Outdoor air dry bulb (wet bulb) temperatures (°C)	**Ambient air dry bulb temperature around the tank (°C)**	**Initial water tank temperature (°C)**	**Heating up of the tank**	**Water tapping flow rate (l/min)**	**Inlet water temperature (°C)**	**Stopping temperature of water tapping (°C)**
7 (6)	20	15	From 15 °C to 45 °C	10	14	15

Table 4-18: Test conditions for performance evaluation

Phase 1: Heating up				Phase 2: Water tapping		
Outdoor air dry bulb (wet bulb) temperatures (°C)	**Ambient air dry bulb temperature around the tank (°C)**	**Initial water tank temperature (°C)**	**Heating up of the tank**	**Water tapping flow rate (l/min)**	**Inlet water temperature (°C)**	**Stopping temperature of water tapping (°C)**
2 (1) 7 (6) 35	20	10	From 10 °C to 60 °C	10	10	10

In addition, EN16147:2011 [12] tests were performed for each refrigerant. The tests consist of the following four principal stages:

A: Heating up period;

B: determination of standby power input;

C: determination of the energy consumption and the coefficient of performance for heating domestic water by using the reference tapping cycles (L);

D: determination of a reference hot water temperature and the maximum quantity of usable hot water in a single tap.

4.2.5.3 Results of the experimental evaluation of R134a alternative refrigerants

4.2.5.3.1 Charge optimization

The initial alternative refrigerant charge was about 1.12 kg (corresponding to 70 % of the initial R134a charge) to perform the charge optimization. Charge optimization was carried out at the conditions. When the refrigerant charge was added (+80 g), new heating up of the tank was done to determine the electricity consumption, the energy content in the water tank, and the pressures and temperatures of the refrigerant circuit. The objective was to identify the performance curve inflection point to determine the optimal charge. The optimal charges obtained are reported in Table 4-19. R513A and R1234yf show optimal charges close to R134a and equivalent performances to R134a. R450A shows an optimal charge close to R134a and slightly lower performance than R134a.

Table 4-19: Charge optimization results (Heating up from 15 °C to 45 °C)

Refrigerant	R134a (baseline)	R513A	R1234yf	R450A
Charge (kg)	1.60	1.60 (0 %)	1.68 (+5 %)	1.68 *(+5 %)*
Heating up time (hh:mm:ss)	03:35:31	03:29:13 *(- 6 min 13 s)*	03:36:19 *(+ 48 s)*	03:59:40 *(+24 min 09 s)*
COP (-)	3.79	3.79 *(0 %)*	3.79 *(0 %)*	3.64 *(- 4.9 %)*

4.2.5.3.2 Heating up performance evaluation

Figure 4-23 presents the results obtained during the heating up of the water tank for three outdoor air temperatures. Table 4-20 provides the values for various parameters. R513A, R1234yf, and R450A show equivalent performances (heating-up times are lower than with R134a, but with R450A, the heating-up times are reached with alternatives are lower than with R134a (-14 K for 450A, -10 K for R1234yf, and -5 K for R513A). At 2(1) °C with R1234yf and R513A, the heating-up times are lower than with R134a, but with R450A, the heating-up times are higher than with R134a.

Table 4-20: Heating up performance evaluation (green color highlights best performance)

Dry air temperature (wet bulb) (°C)	**2(1)**				**7(6)**				**35**			
Refrigerant	**R134a (base)**	**R513A**	**R1234yf**	**R450A**	**R134a (base)**	**R513A**	**R1234yf**	**R450A**	**R134a (base)**	**R513A**	**R1234yf**	**R450A**
Heating up time (hh:mm:ss)	11:55:03	**10:59:30 *(-56min)***	11:08:24 *(-47min)*	13:29:15 *(+94min)*	06:35:03	**06:23:59 *(-11min)***	06:49:34 *(+14min)*	07:37:35 (+73min)	**03:42:55**	**03:42:58 *(=)***	03:55:24 *(+12min)*	03:55:08 *(+12min)*
Electric energy consumption (Wh)	5 760	5 568 *(-3.4 %)*	**5 446 *(-5.5 %)***	5997 (+4.1 %)	3 618	3 622 *(+0.1 %)*	3 685 *(+1.8 %)*	3802	2 441	2 478 *(+1.5 %)*	2453 *(+0.5 %)*	**2357 *(-3.4 %)***
Stored energy (Wh)	11 718	11 704 *(-0.1%)*	11 732 *(+0.1 %)*	11659 *(-0.5 %)*	11 563	11 577 *(+0.1%)*	11 623 *(+0.5 %)*	11 523	11 538	11 484 *(-0.5 %)*	11525 *(-0.1 %)*	11345 *(-1.6 %)*
COP (-)	2.0	2.1 *(+3.3 %)*	**2.2 *(+5.9 %)***	1.94 *(-3.0 %)*	**3.2**	**3.2 *(=)***	3.2 *(-1.3 %)*	3.0 (-6 %)	4,7	4,6 *(-2.0 %)*	4,7 *(-0.6 %)*	**4.8 *(+2.1 %)***
Maximal discharge temperature (°C)	83.9	78.9 *(-5.0 K)*	73.9 *(-10.0 K)*	69.6 *(-14.3 K)*	85,3	78.9 *(-6.5 K)*	74.4 *(-10.9 K)*	69.8	90,8	86.7 *(-4.2 K)*	81.7 *(-9.1 K)*	78.2 *(-12.6 K)*

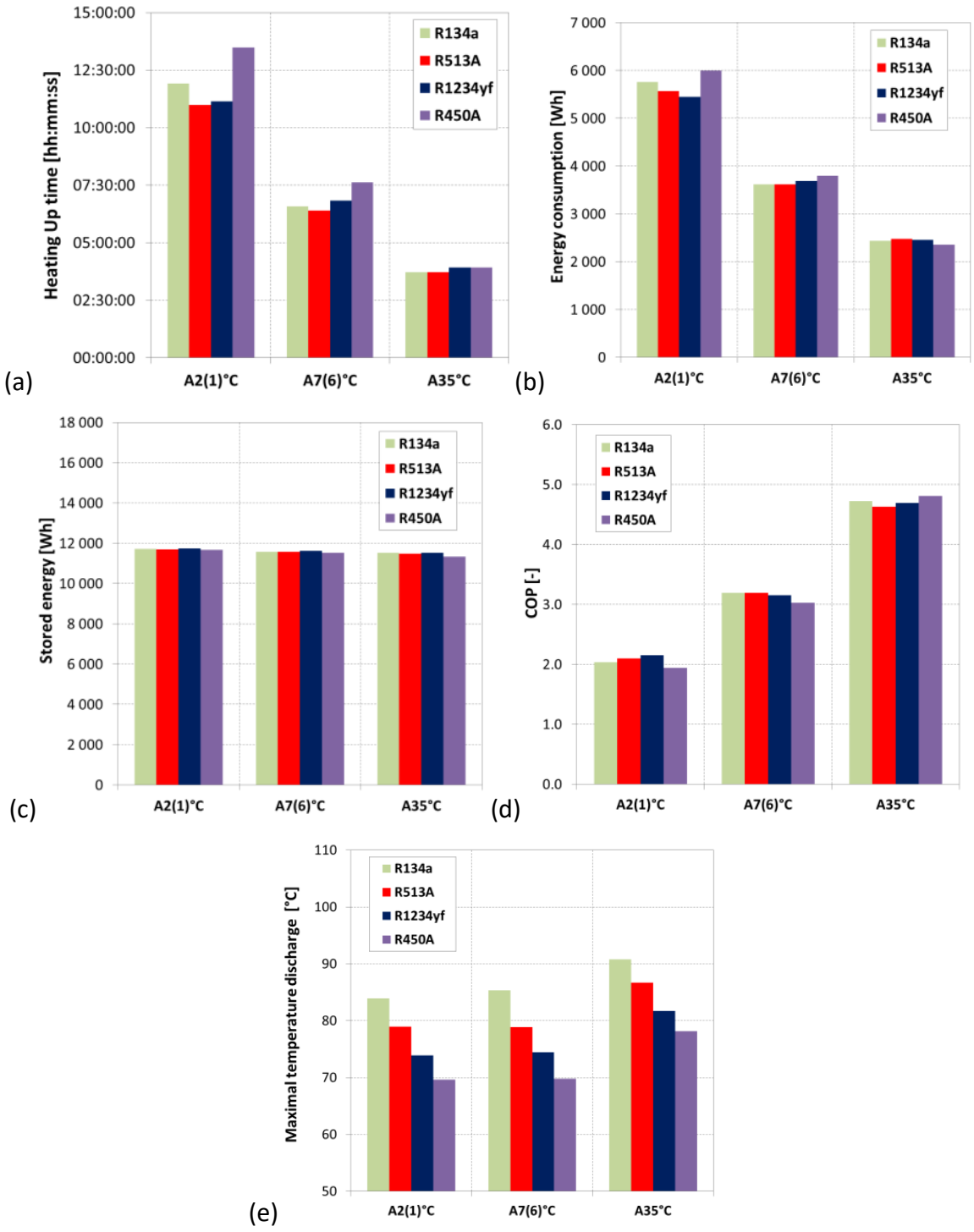

Figure 4-23: Heating up performance evaluation: (a) Heating up time; (b) Electric energy consumption; (c) Water energy content; (d) COP; (e) Maximal discharge temperature

4.2.5.3.3 EN 16147:2011 tests

Table 4-21 provides the main results of the EN 16147:2011 tests.

Table 4-21: Main results of the EN 16147:2011 tests

Test conditions						
Refrigerant			**R134a**	**R513A**	**R1234yf**	**R450A**
Refrigerant charge	kg		**1.6**	**1.6**	**1.68**	**1.68**
Outdoor air temperature (DB / WB)	°C / °C		**7(6)**	**7(6)**	**7(6)**	**7(6)**
Size of tapping cycle	-		**L**	**L**	**L**	**L**
DHW set point (fixed on the product)	°C		**55**	**55**	**55**	**55**
Performances in accordance with standard EN16147:2011						
Heating up time	-	t_h	5:55:30	5:47:15	6:10:21	6:34:54
Heating up energy input	Wh	W_{eh}	3214	3179	3222	3183
Determination of Standby power						
Duration of the last on-off cycle to determine the standby power input	-	t_{es}	27:01:18	26:54:36	27:12:54	24:59:03
Energy input during last on-off cycle	Wh	W_{es}	961	926	949	918
Standby power input	W	P_{es}	36	34	35	37
Determination of COP						
Total useful heat energy during the whole tapping cycle	Wh	Q_{TC}	11655	11655	11655	11655
Time period of test cycle	-	t_{TTC}	43h 52m 3s	43h 36m 17s	44h 9m 15s	42h 10m 7 s
Measured electrical energy consumption during the whole tapping cycle	Wh	$W_{EL\text{-}M\text{-}TC}$	4940	4774	4852	4991
Electrical energy consumption of fans or liquid pumps	Wh	$W_{EL\text{-}CORR}$	0.00	0.00	0.00	0.00
Calculated heat energy producted by electricity during the whole tapping cycle	Wh	$Q_{EL\text{-}TC}$	56	60	58	53
Total electrical energy consumption during the whole tapping cycle	Wh	$W_{EL\text{-}TC}$	4289	4159	4208	4376
Coefficient of performance	**-**	COP_{DHW}	**2.72**	**2.80**	**2.77**	**2.66**
Reference hot water temperature	°C	θ'_{WH}	53.1	53.1	53.1	53.1
Maximum quantity of usable hot water	liters	$Vmax$	282.1	292.6	292.2	290.7

The normative tests provide the same conclusions as the heating-up performance tests, i.e., R513A, R1234yf, and R450A show equivalent performances to those of R134a.

4.2.5.3.4 Performance verification

To ensure that alternative refrigerants did not damage the HPWH, a heating up with the initial R134a charge (1.6 kg) was performed. The performance gaps obtained for heating up time and electric energy consumption are quite small, +7 min 21 s and +1.5 %, respectively, and within the measurement uncertainty. We can conclude that there was no notable damage to the heat pump after the use of both alternative refrigerants.

According to these results, R513A and R1234yf might be considered as alternatives to R134a without performance impact, and R450A might be considered as alternatives to R134a, but with a decrease of the thermal capacity of the system (Heating up time longer).

4.2.6 Conclusions

A total of 10 low-GWP alternative refrigerants were evaluated with not less than 130 performance tests. The principal results of the study are summarized below.

R459A, R454B, R447A, HPR2A, and R32 were investigated for the drop-in replacement of R410A in a 10 kW air-to-water reversible heat pump. R410A replacement by HFC/HFO mixtures showed no particular problem, and the performance obtained is, aside from some very few exceptions,

almost equivalent (+/- 10 %) to that of R410A. Furthermore, in operating limit conditions, the heat pump worked normally with alternative refrigerants HFC/HFO mixtures. With R32, the operating map of the heat pump would be decreased because of the high discharge temperatures reached. R454B and R459A showed the best performances.

R454C and R455A were evaluated as a possible alternative to R407C in a 3 kW water-to-air reversible heat pump. The R454C seems to be more suited to replacing the R407C for a reversible machine, since the performance is almost equivalent to that of the R407C in both operating modes. For the heating-only mode, R455A achieves the best results (+ 6.1 % to + 8.6 % heating capacities and equivalent COP). R454C and R455A can therefore be considered as alternatives for R407C.

R1234yf, R513A, and R450A were tested for replacing R134a in a split heat pump water heater with a water tank of 200 liters. They showed equivalent performances to R134a. The discharge temperatures reached with alternatives are lower than those with R134a, of -14K for R450A, -10 K for R1234yf and -5 K for R513A. R513A and R1234yf might be considered as alternatives to R134a without significant performance impact, and R450A might be considered as alternatives to R134a, but with a decrease in the thermal capacity of the system (Heating up time longer).

With the exception of R450A and R513A, which have a A1 safety class, all the others alternative, R1234yf, R459A, R454B, R447A, HPR2A, R32, R454C and R455A, have an A2L safety class. It means that a new risk must be handled: flammability. Using these alternative refrigerants will require a complete study of the risks, sizing, and compatibility.

Finally, what are the most promising low-GWP refrigerants for replacing the HFC commonly used in heat pumps? Figure 4-24 tries to answer to this question.

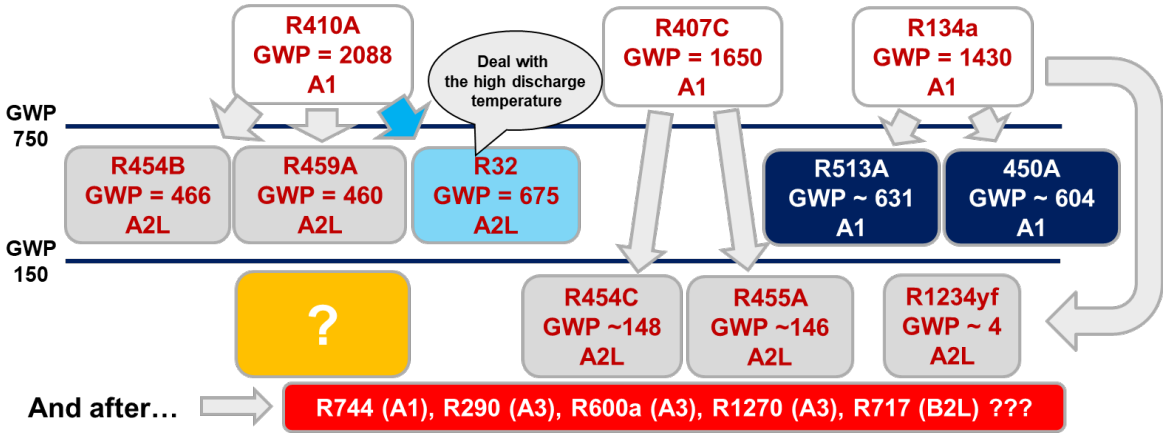

Figure 4-24: Most promising Low-GWP refrigerants

Long-term alternatives (GWP<150) exist for R407C and R134a, but for R410A only transition alternatives are available (150<GWP<750). Other solutions need to be studied, especially natural fluids.

These experimental results will be useful to the HVAC community for selecting the most promising refrigerant candidates to replace R410A, R134a and R407C. Beyond drop-in, improving the thermal performances of the heat pumps would require component optimization. For example, it would be necessary to re-size and replace the expansion valve, especially when a calibrated orifice or a capillary tube is used, or to optimize the design of the heat exchanger(s).

4.2.7 References

[1] Performance ranking of refrigerants with low global warming potential - Kedzierski, M. A., Brown, J. S., and Koo, J. - Science and Technology for the Built Environment, 2015, (21), 207-219.

[2] Assessment of DR-55 as a Drop-In Replacement for R410A - Shen B., Abdelaziz O., Liudahl L. - (2333) - 16th International Refrigeration and Air Conditioning Conference at Purdue, July 11-14, 2016. Purdue, United States.

[3] Update on Phase II of the AHRI Low-GWP Alternative Refrigerants Evaluation Program (Low-GWP AREP) - Amrane, K. and Wang X. - *Technical Forum on Research Projects for Alternative Refrigerants in High Ambient Countries.* 31 October 2015, Dubai, UAE.

[4] AHRI Low Global Warming Potential Alternative Refrigerants Evaluation Program (Low-GWP AREP) – Summary of Phase II Testing Results - (2064) - Wang X. and Amrane K. - *16th International Refrigeration and Air Conditioning Conference at Purdue, July 11-14, 2016.* Purdue, United States.

[5] Evaluation of R410A refrigerant alternatives in a residential reversible air-to-water heat pump - (2103) - Pardo, P., Charbonnier, L. and Mondot, M. - *16th International Refrigeration and Air Conditioning Conference at Purdue, July 11-14, 2016.* Purdue, United States.

[6] Performance Evaluation of Heat Pump System using R32 and HFO-mixed Refrigerant in High Ambient Temperature - (2408) - Taira S., Minamida T., Haikawa T. and Ohta F. - (2016) - *16th International Refrigeration and Air Conditioning Conference at Purdue, July 11-14, 2016.* Purdue, United States.

[7] Participants Handbook: ARHI Low-GWP Alternative refrigerants evaluation program (Low-GWP AREP) - Amrane, K. - 2015 - Retrieved from http://www.ahrinet.org/site/1/Home.

[8] REFPROP V10.0, Reference Fluid Thermodynamic and Transport Properties - Lemmon E.W., Bell I.H., Huber M.L. and McLinden M.O. - 2018.

[9] R404A, R134a and R410A replacement - De Bernardi, J. - *Honeywell master presentation,* June 2014.

[10] Novel Reduced GWP Refrigerants for Stationary Air Conditioning - Leck T. J., Hughes J., Naicker P. and Hydutsky B. - *15th International Refrigeration and Air Conditioning Conference at Purdue, July 11-14, 2014.* Purdue, United States.

[11] Air conditioners, liquid chilling packages and heat pumps for space heating and cooling and process chillers, with electrically driven compressors - Part 2: Test conditions and Part 3: Test methods – EN 14511:2013 – 2013.

[12] Heat pumps with electrically driven compressors Testing and requirements for marking of domestic hot water units - NF EN 16147:2011 - 2011.

4.3 Case studies and design guidelines for optimization components

Prepared by:

Pierre PARDO[1]*

[1]CETIAT, Centre Technique des Industries Aérauliques et Thermiques, HVAC systems department, Villeurbanne, France

***Corresponding author e-mail:** pierre.pardo@cetiat.fr

4.3.1 Summary

This report presents a study carried out by the CETIAT on finned tube heat exchangers using low GWP refrigerants. This work has already been presented during the International Congress of Refrigeration 2019 (Pierre PARDO, Nicolas GAILLARD, Michèle MONDOT, Experimental and numerical study of heat transfer in evaporation and condensation with R410A, R32 and R454B in a finned tube heat exchanger, Manuscript ID: 1439 DOI: 10.18462/iir.icr.2019.1439).

The progressive phase-out of HFCs and their replacement by the 4th generation of refrigerants require identifying the performance of these alternative refrigerants in heat exchangers. This study aimed to assess the heat transfer performance during evaporation and condensation of R410A, R454B, and R32 in a finned tube heat exchanger. A 30 kW experimental setup was built to assess the heat exchanger performance with these three refrigerants. For each refrigerant, 6 tests were carried out in evaporation and 5 tests in condensation. During the tests, the energy balance between the thermal capacities measured on the air and refrigerant sides was found to be less than 5%, which confirmed a good accuracy of measurements. A good agreement (+/-2.5%) between experimental data and simulations was allowed using EVAP-COND software to compare the performance of the same heat exchanger design with the 3 refrigerants. The simulations show that the same finned tube heat exchanger design can be used for R410A and R454B, but a design optimization will be necessary with R32.

Keywords: Low GWP Refrigerants, Finned Tube Heat Exchanger, R410A, R32, R454B

4.3.2 Introduction

The chemical industry is now offering new refrigerants with low GWP. Some of these refrigerants will be tomorrow's solutions, and HVAC manufacturers have to be ready to use them. Studies conducted on this transition essentially dealt with the thermal performances of low GWP refrigerants in existing equipment with drop-in tests or soft optimization tests (Amrane, 2015; Wang and Amrane, 2016; Pardo and Mondot, 2018). Some also examined the compatibility between low GWP refrigerants and materials (Majurin et al., 2014). Studies on heat transfer of low GWP refrigerants in evaporation and in condensation have been published (Azzolin et al., 2016; Del Col et al., 2010; Diani et al., 2014; Diani et al., 2015; Jige et al., 2016; Jige et al., 2017; Longo et al., 2018a; Longo et al., 2018b). Most of these works focused on the heat transfer coefficient in evaporation or in condensation in smooth tubes, microchannels and microfin tubes. The evaluation of the heat transfer coefficient is essential for the heat exchanger design.

The objectives of this work are to assess experimentally the thermal performance, capacity, and pressure drop, in condensation and in evaporation, of R32 and R454B, as alternatives to R410A, in a finned tube heat exchanger and to use a reliable software tool for performance comparison of the refrigerants.

The paper is divided into three parts:

- presentation of the main refrigerant properties;
- experimental investigation: method and results;
- numerical investigation: validation of EVAP-COND software (Domanski and Yashar, 2016) and simulations in evaporation and condensation modes.

4.3.3 Refrigerant properties

The choice of the alternative refrigerants to R410A is based on the result analysis of the AHRI Low GWP AREP program (Wang and Amrane, 2016) and on the experimental results of drop-in tests previously carried out in an air-to-water heat pump by CETIAT (Pardo and Mondot, 2018). Table 4-22 presents the main properties of the selected refrigerants. The data source is the software REFPROP V10 (Lemmon et al., 2018).

Table 4-22: Refrigerant properties

Refrigerant	Composition	GWP_{100}	Latent heat (kJ/kg) (at 0 °C)	Critical temperature (°C)	Normal boiling point (°C)	Glide (K)	Safety class
R410A	R32/R125 (50/50%w)	2088	221.3	70.2	-51.6	0.1	A1
R32	R32 (100%w)	675	315.3	78.0	-52.0	0	A2L
R454B	R32/R1234yf (68.9/31.1%w)	466	260.9	78.1	-50.4	1.3	A2L

Alternative refrigerants have a lower GWP than R410A, -67% for R32 and -78% for R454B. R32 is a pure refrigerant, and R454B is a mixture composed of R32 (~69%w) and R1234yf (~31%w). The phase change enthalpies of R454B and R32 are higher than that of R410A by +18% and +42%, respectively. The safety class of alternative refrigerants is A2L, which means they have low flammability and are non-toxic. The saturation properties (pressure-temperature) are shown in Figure 4-25. The three refrigerants have equivalent saturation properties. R454B remains slightly less volatile than R410A and R32.

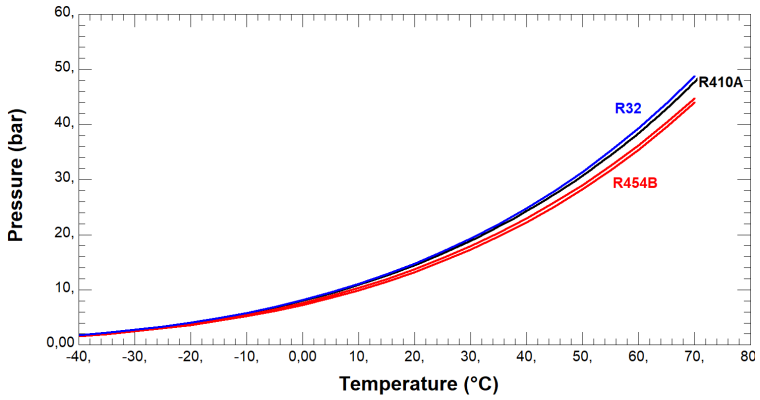

Figure 4-25: Saturation properties: Pressure-Temperature

4.3.4 Experimental investigation

4.3.4.1 Finned tube heat exchanger description

The main characteristics of the finned tube heat exchanger are presented in Figure 4-26. The finned tube heat exchanger was designed to operate either as an evaporator or as a condenser in a reversible air-to-water heat pump for an optimal heating performance. During tests, two flow patterns were thus used (see Figure 4-26d):

- Evaporation mode: counter-current;
- Condensation mode: co-current.

a)

ROW DATA	
Number of rows	3
Number of tubes per row	32
Number of circuits	8
FIN DATA	
Fin type	Louver
Pitch	2,5 mm
Thickness	0,08 mm
Material	Aluminium
TUBE DATA	
Tube length	813 mm
Inner diameter	7,81 mm
Outer diameter	8,37 mm
Tube pitch	25,5 mm
Depth row pitch	20 mm
Inner surface	Smooth
Material	Copper

b) c)

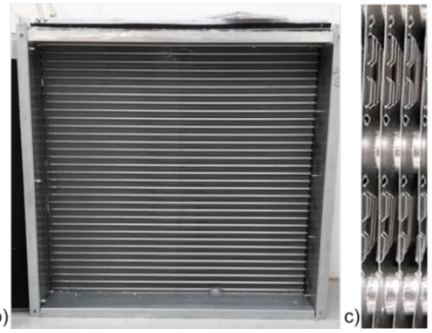

d)

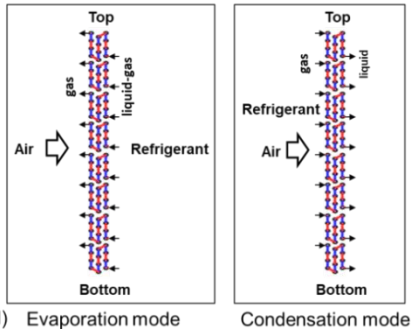

Figure 4-26: Main characteristics of the tested finned tube heat exchanger: a) Geometry characteristics; b) Overview photography; c) Fins close-up; d) Flow patterns

In evaporation mode, the refrigerant flows through a distributor at the upstream side of the heat exchanger, in which a diaphragm is placed. This element generates an additional pressure drop downstream of the expansion device. Then, the distributor is connected to eight capillary tubes which each feed a circuit. At the outlet, the eight circuits are connected to a collector. In condensation mode, the refrigerant flows in the other way with a bypass of the diaphragm through a non-return valve; the circuit thus generates less pressure drop than in evaporation mode (see Figure 4-28).

4.3.4.2 Experimental set-up

A 30 kW thermodynamic loop was designed and built to test the finned tube heat exchanger. It is composed of an inverter driven compressor, an oil separator, a plate heat exchanger and a manual expansion device. Pt100 contact probes (-20 to 100°C, +/-0.1°C) and pressure transducers (0-

40 barg, +/-0.01 barg) are installed at the inlet and outlet of each component of the refrigerating circuit. In addition, a Coriolis mass flow meter (0-720 kg/h, +/-1%) in the liquid line, at the outlet of the condenser, allows measuring the refrigerant flow. This loop allows controlling the test conditions at the inlet of the finned tube heat exchanger on the refrigerant side. On the air side, the finned tube heat exchanger is installed between straight ducts of 2500 mm length, having the same rectangular section as the heat exchanger frontal surface (813 mm × 813 mm) and a 20 mm thick thermal insulation (λ = 0.022 W/m.K). The inlet air is the ambient air of a climatic room which is controlled in temperature and humidity by an air handling unit. The air volumetric flow rate is adjusted and measured thanks to a multi-nozzle chamber coupled to a fan (0-6000 m^3/h, +/-3.5%). Pt100 probes (-20 to 100°C, +/-0.1°C), mirror hygrometers (-20 to 60°C, +/-0.3°C) and Pitot probes (0-100 Pa, +/-1Pa) are placed upstream and downstream to measure the air-dry bulb and the dew point temperatures and the pressure drop, respectively. The schematic diagram in Figure 4-27 shows the installation and the instrumentation in evaporation mode.

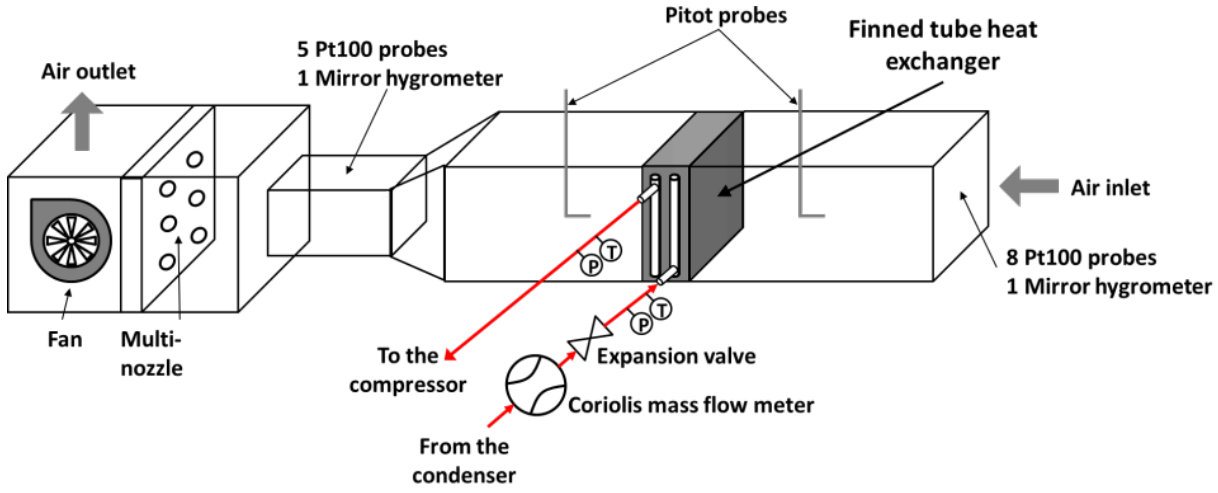

Figure 4-27: Schematic diagram of the installation and the instrumentation in evaporation mode

In addition, the inlet and outlet of the finned tube heat exchanger were instrumented with pressure transducers and Pt100 contact probes. The fifth circuit from the top of the finned tube heat exchanger was instrumented with 3 pressure transducers (red squares) and 10 Pt100 contact probes (blue hexagons) (see Figure 4-28).

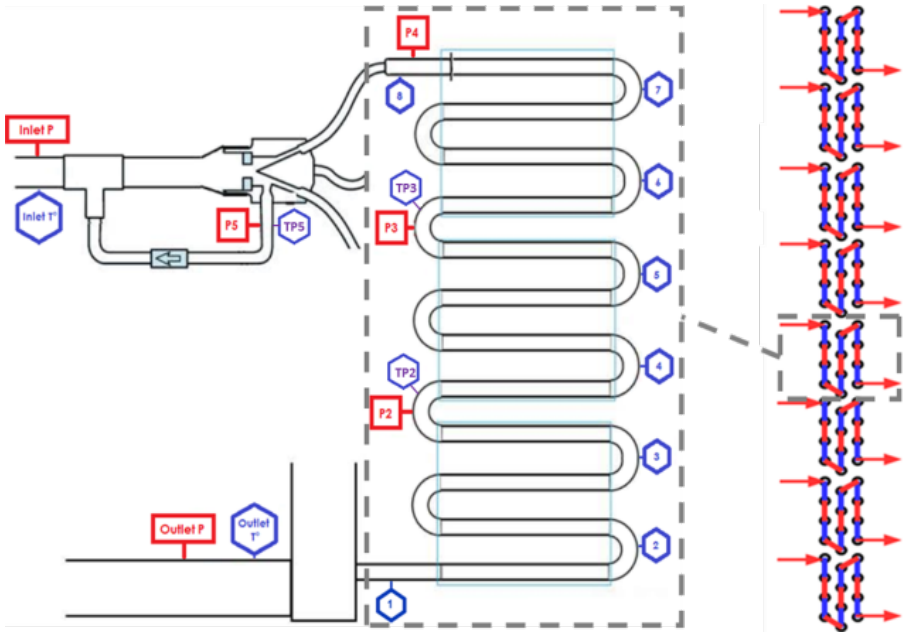

Figure 4-28: Specific instrumentation placed at inlet/outlet and on the 5th circuit from the top of the finned tube heat exchanger

4.3.4.3 Test conditions

4.3.4.3.1 Evaporation mode

The test conditions in evaporation mode are shown in Table 4-23.

Table 4-23: Test conditions in evaporation mode

Run	Flow	Air	Air dry bulb temperature (wet bulb temperature) (°C)	Air frontal velocity ($m.s^{-1}$)	Refrigerant mass flow rate ($kg.h^{-1}$)	Refrigerant liquid temperature (°C)
1	Counter-current	Dry	20(10)	2.25	230	30
2	Counter-current	Dry	20(10)	2.25	270	30
3	Counter-current	Dry	20(10)	2.25	330	30
4	Counter-current	Wet	16(14)	2.25	230	30
5	Counter-current	Wet	16(14)	2.25	270	30
6	Counter-current	Wet	16(14)	2.25	330	30

Two air-dry and wet bulb conditions are defined. For each, the refrigerant flow is set at three different values. To obtain an air frontal velocity of 2.25 $m.s^{-1}$, the inlet volumetric air flow rate is adjusted close to 5350 $m^3.h^{-1}$ (+/-50 $m^3.h^{-1}$). 2.25 $m.s^{-1}$ is the maximal frontal air velocity reachable by the experimental set-up, due to the fan downstream of the multi-nozzle chamber.

4.3.4.3.2 Condensation mode

The test conditions in condensation mode are shown in Table 4-24.

Table 4-24: Test conditions in condensation mode

Run	Flow	Air	Air dry bulb temperature (wet bulb temperature) (°C)	Air frontal velocity ($m.s^{-1}$)	Refrigerant mass flow rate ($kg.h^{-1}$)	Refrigerant inlet condenser temperature (°C)
1	Co-current	-	30(-)	2.15	230	80
2	Co-current	-	30(-)	2.15	270	80
3	Co-current	-	30(-)	2.15	330	80
4	Co-current	-	30(-)	2.15	360	80

One air condition is tested with four refrigerant flow rates. To obtain an air frontal velocity of 2.15 m/s, the inlet volumetric air flow rate is adjusted close to 5115 $m^3.h^{-1}$ (+/-50 $m^3.h^{-1}$). The frontal air velocity is lower than in evaporation because the air-specific volume at the inlet of the heat exchanger is slightly higher: 0.9 against 0.85 (at 16°C) $m^3_{wet\_air}.kg_{dry\_air}^{-1}$. Thus, 2.15 $m.s^{-1}$ is the maximal reachable frontal air velocity.

4.3.4.4 Experimental results

In this section, the evaporating or condensing temperatures, the thermal capacities and the pressure drops measured during the tests are presented.

4.3.4.4.1 Evaporation mode

During the evaporation tests, the heat balance between the thermal capacities measured on the air and refrigerant sides is comprised between:

- 0.4% and 2.5% in dry air condition;
- 3.4% and 9.3% in wet air condition.

Three tests with wet air (among a total of nine) have a heat balance between 6.1% and 9.3%. There is only one dew point temperature measurement in the downstream duct against five for the dry temperature (mean value from 5 Pt100 probes). It can thus be considered that the dew point temperature measurement probably generates these heat balance deviations. Nevertheless, the measurements can be considered as reliable enough in the context of this study.

The evaporating temperatures, the superheating (SH), the cooling capacity, and the pressure drop (P4 – Outlet P; see Figure 4-28) are presented in Table 4-25 for the three refrigerants.

Table 4-25: Main results measured on the refrigerant side in evaporation mode

Refrigerant	Run	Evaporating temperature (°C)		SH (K)	Cooling capacity (kW)	Pressure drop (kPa)
		Bubble point	Dew point			
R410A	1	2.2	1.4	16.6	12.2	22
	2	1.1	-0.3	17.6	14.3	36
	3	-0.7	-2.8	18.5	17.5	52
	4	3.4	2.6	11.7	11.9	20
	5	0.4	-1.0	15.1	14.1	37
	6	-0.5	-2.7	16.0	17.3	52
R454B	1	1.8	0.4	16.7	14.6	33
	2	0.5	-1.3	17.3	17.0	46
	3	-0.3	-3.3	15.6	20.8	69

	4	0.4	-1.1	15.2	14.3	36
	5	0.2	-1.8	15.2	17.1	47
	6	0.3	-2.7	14.6	20.6	69
R32	1	2.2	1.0	12.7	17.4	29
	2	-3.7	-4.7	20.9	21.1	59
	3	-3.5	-7.1	12.5	25.1	78
	4	2.2	1.0	11.0	17.5	29
	5	0.6	-1.4	12.4	20.6	46
	6	-1.7	-5.1	14.0	25.2	77

It should be noted that the evaporating temperatures of the three refrigerants are not the same. The differences can reach up to 5 K (see runs 2, 3 and 4). This is due to the difficulty in adjusting this parameter during the test. Some differences in cooling capacity are due to better heat transfer coefficient values, and some are due to large temperature differences between air and refrigerant. Similarly, on pressure drop, most of the increase in pressure drop for R32 and R454B seems to be due to lower evaporation temperature (and pressure), so lower density vapor and higher vapor velocities for the same mass flow. This means that we cannot directly conclude the benefit of using one refrigerant compared to another.

4.3.4.4.2 Condensation mode

During the condensation tests, the heat balance between the thermal capacities measured on the air and refrigerant sides is comprised of between 0.5% à 2.1%. The measurements are reliable.

The condensing temperatures, the subcooling (SC), the heating capacity, and the pressure drop (Outlet P – P4; see Figure 4-28) are presented in Table 4-26 for the three refrigerants.

Table 4-26: Main results measured on the refrigerant side in condensation mode

Refrigerant	Run	Condensing temperature (°C)		SC (K)	Heating capacity (kW)	Pressure drop (kPa)
		Dew point	Bubble point			
R410A	1	46.6	46.3	6.2	13.31	18
	2	48.3	48.1	6.6	15.29	18
	3	50.2	49.9	4.8	17.8	23
	4	51.1	50.7	4.0	19.25	21
R454B	1	50.3	48.5	7.3	15.29	16
	2	52.1	50.3	7.7	17.34	19
	3	53.8	52.0	6.2	20.39	20
	4	55.0	53.2	5.9	21.88	22
R32	1	49.4	49.3	4.4	17.78	16
	2	51.5	51.3	4.3	20.10	17
	3	54.0	53.8	3.3	23.44	20
	4	56.3	56.1	5.7	25.45	21

As previously, the condensing temperatures of the three refrigerants do not have the same value. The differences can reach up to 5 K. We cannot directly conclude on the benefit of using one refrigerant in comparison to another.

4.3.5 Numerical investigation

4.3.5.1 Software validation

This part aims to compare the experimental results with the results of the EVAP-COND software. The geometrical parameters of the finned tube heat exchanger and the inlet operating conditions have been used as input data in the software. The 30 experimental tests were simulated and compared. The calculated versus experimental capacities of R410A, R454B, and R32, in evaporation and condensation modes, are plotted in Fig. 5.

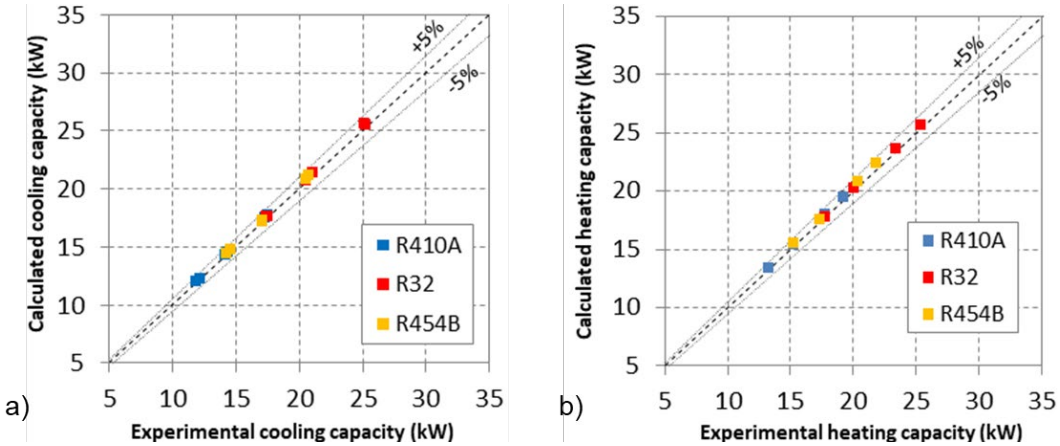

Figure 4-29: Calculated capacity versus experimental capacity of R410A, R454B and R32, for both modes: a) Evaporation mode; b) Condensation mode

According to Figure 4-29, the comparison shows that the EVAP-COND software is a reliable tool for simulating the thermal capacity of finned tube heat exchangers. The maximal deviation observed is less than 2.5%. As a reminder, the fifth circuit from the top of the finned tube heat exchanger was instrumented with 10 Pt100 contact probes and 3 pressure transducers. The comparisons between the simulated and the experimental temperature and pressure evolutions along the 5th circuit of run 1, in evaporation and condensation, are shown in Figure 4-30 and Figure 4-31, respectively. The horizontal axis refers to the inlet and outlet of each of the 12 tubes of the circuit.

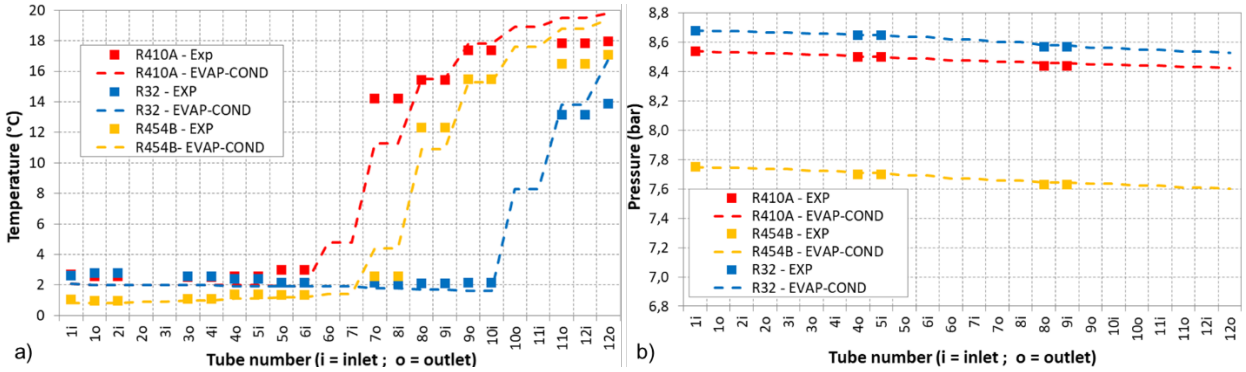

Figure 4-30: Calculated and experimental temperatures and pressures along the 5th circuit in evaporation: a) Refrigerant temperature; b) Refrigerant pressure

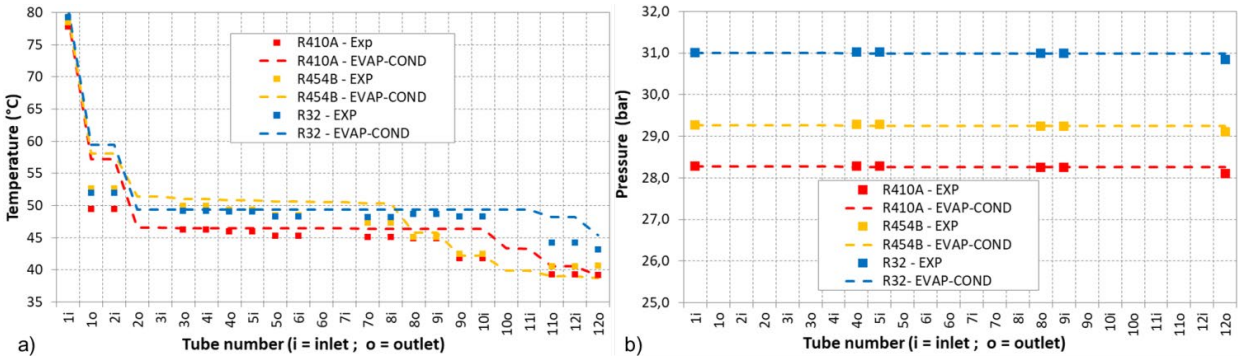

Figure 4-31: Calculated and experimental temperatures and pressures along the 5th circuit in condensation: a) Refrigerant temperature; b) Refrigerant pressure

The temperature and pressure evolutions of the three refrigerants in the simulated circuit are close to those observed during experimental tests. The same conclusions are drawn from all other runs of the tests (not presented in detail in this paper). We can conclude that EVAP-COND software is a reliable tool for designing the finned tube heat exchanger; however, its robustness has not been fully validated in this study. Since most of the HFC alternatives have a high-temperature glide, comparing experimental results obtained with a higher-temperature glide refrigerant (>5 K) and the EVAP-COND simulations could be interesting.

4.3.5.2 Numerical analysis

EVAP-COND software is then used to simulate the performance in evaporation and condensation modes of the same heat exchanger design with different refrigerants. For that purpose, the refrigerant mass flow rate is not fixed as it was for the experimental approach.

In evaporation mode, the SC1 condition of the NF EN 328 standard (see Table 4-27) is used with an air frontal velocity of 2.25 $m.s^{-1}$. The main results are presented in Table 4-28.

Table 4-27: SC1 condition of the NF EN 328 standard

Air dry bulb temperature (°C)	Dew point temperature (°C)	Evaporating temperature (Dew point) (°C)	Superheating (K)	Refrigerant liquid temperature (°C)
10	< -2	0	6.5	30

Table 4-28: Main simulation results: Evaporation mode – SC1

Refrigerant	Evaporating temperature (°C)		Refrigerant mass flow rate ($kg.h^{-1}$)	Cooling capacity (kW)	Pressure drop (kPa)
	Bubble point	Dew point			
R410A	0.2	0	195	9.7	8.7
R32	0.1	0	125 (-36%)	9.3 (-5%)	5.2 (-40%)
R454B	-0.7	0	170 (-13%)	10.3 (+5%)	8.7 (0%)

Compared to R410A, R454B shows a higher cooling capacity (+5%) and an equivalent pressure drop. In comparison to R410A, R32 shows a lower cooling capacity (-5%), but also a lower mass flow rate (-36%) and a lower pressure drop (-40%).

In condensation mode, the SC1 condition of the NF EN 327 standard (see Table 4-29) is used with an air frontal velocity of 2.15 $m.s^{-1}$. The main results are presented in Table 4-30.

Table 4-29: SC1 condition of the NF EN 327 standard

Air dry bulb temperature (°C)	Condensing temperature (Bubble point) (°C)	Subcooling (K)	Superheating (K)
25	40	< 3	40

Table 4-30: Main simulation results: Condensation mode – SC1

Refrigerant	Condensing temperature (°C)		Refrigerant mass flow rate ($kg.h^{-1}$)	Heating capacity (kW)	Pressure drop (kPa)
	Bubble point	Dew point			
R410A	39.9	40.1	212	12.9	2.4
R32	40.0	40.0	151 (-29%)	12.7 (-1%)	1.8 (-25%)
R454B	39.9	41.2	186 (-12%)	13.3 (+3%)	2.4 (0%)

Compared to R410A, R454B shows a slightly higher heating capacity (+3%) and an equivalent pressure drop. In comparison to R410A, R32 shows an equivalent heating capacity (-1%), a lower mass flow rate (-29%), and a lower pressure drop (-25%).

To replace R410A, the same finned tube heat exchanger could be designed with R454B, and design optimization will be necessary for R32.

4.3.6 Conclusions

In the first part of this study, the thermal performances of R410A, R32, and R454B were measured in a finned tube heat exchanger, in condensation, and in evaporation. 30 tests were carried out. In the second part of the study, the experimental results were used to validate the simulation results from the EVAP-COND software. The differences between experimental and calculated capacities are less than 2.5% for all tests. The temperature and pressure evolutions of the three refrigerants in the simulated circuit are also close to those observed during experimental tests. These comparisons for a pure, a quasi-azeotrope, and a small temperature glide (<2 K) refrigerants allow considering EVAP-COND software as a reliable tool for the simulation of finned tube heat exchangers. The simulations of the same heat exchanger design with the 3 refrigerants show that the same design of finned tube heat exchanger can be used for R410A and R454B, but a design optimization will be necessary with R32.

4.3.7 References

Amrane, K., 2015. Participants Handbook: ARHI Low-GWP Alternative refrigerants evaluation program (Low-GWP AREP). Retrieved from http://www.ahrinet.org/site/1/Home.

Azzolin, M., Bortolin, S., Del Col, D., 2016. Flow boiling heat transfer of a zeotropic binary mixture of new refrigerants inside a single microchannel. Int. J. Thermal Sciences 110, 83-95.

Del Col, D., Torresin, D., Cavallini, A., 2010. Heat transfer and pressure drop during condensation of the low GWP refrigerant R1234yf. Int. J. Refrigeration 33, 1307-1318.

Diani, A., Tamura, M.T., Mancin, S., Barbosa, J., Rossetto, L., 2014. R1234yf flow boiling heat transfer inside a 3.4 mm ID microfin tube. 15th International Refrigeration and Air Conditioning Conference at Purdue, paper number 2460.

Diani, A., Mancin, S., Cavallini, A., Rossetto, L., 2015. R1234ze(E) flow boiling heat tranfer and pressure drop inside a 2,4 mm microfin tube. 24th International Congress of Refrigeration, Yokohama, paper number 549.

Domanski, P. A., Yashar, D. A., 2016. EVAP-COND V4.0, Simulation models for finned-tube heat exchangers with circuitry optimization. Retrieved from https://www.nist.gov/services-resources/software/evap-cond.

Jige D., Sagawa, K., Inoue, N., 2016. Flow boiling heat transfer characteristics of R32 inside a horizontal small-diameter microfin tube. 16th International Refrigeration and Air Conditioning Conference at Purdue, paper number 2371.

Jige D., Sagawa, K., Inoue, N., 2017. Effect of tube diameter on boiling heat transfer and flow characteristic of refrigerant R32 in horizontal small-diameter tubes. Int. J. Refrigeration 76, 206-218.

Lemmon, E.W., Bell, I.H., Huber, M.L., McLinden, M.O., 2018. REFPROP, Reference Fluid Thermodynamic and Transport Properties, Database 23, V10.

Longo, G. A., Mancin, S., Righetti, G., Zilio, C., 2018a. R134a and its low GWP substitutes R1234yf and R1234ze(E) flow boiling inside a 4 mm horizontal smooth tube. 17th International Refrigeration and Air Conditioning Conference at Purdue, paper number 2204.

Longo, G. A., Mancin, S., Righetti, G., Zilio, C., 2018b. R134a and its low GWP substitutes R1234yf and R1234ze(E) condensation inside a 4 mm horizontal smooth tube. 17th International Refrigeration and Air Conditioning Conference at Purdue, paper number 2205.

Majurin, J., Gilles, W., Staats, S.J., 2014. Material Compatibility of HVAC&R System Materials with Low GWP Refrigerants. 15th International Refrigeration and Air Conditioning Conference at Purdue, paper number 2132.

Pardo, P., Mondot, M., 2018. Experimental evaluation of R410A, R407C and R134a alternative refrigerants in residential heat pumps. 17th International Refrigeration and Air Conditioning Conference at Purdue, paper number 2498.

Wang, X., Amrane, K., 2016. AHRI low global warming potential alternative refrigerants evaluation program (Low-GWP AREP) – summary of phase II testing results. 16th International Refrigeration and Air Conditioning Conference at Purdue, paper number 2064.

4.4 Overall conclusions

The conclusions of this study highlight several important points:

The thermal performances of the refrigerants R410A, R32, and R454B were measured in a finned tube heat exchanger, both in condensation and evaporation. The experimental results were used to validate simulations conducted with the EVAP-COND software, showing differences of less than 2.5% between experimental and calculated capacities, confirming the reliability of this simulation tool.

Ten low-GWP alternative refrigerants were evaluated, with over 130 performance tests conducted. The principal results are:

- For the replacement of R410A in a 10 kW air-to-water reversible heat pump, HFC/HFO mixtures like R459A, R454B, R447A, HPR2A, and R32 showed performances almost equivalent to those of R410A, with R454B and R459A showing the best performances.
- For the replacement of R407C in a 3 kW water-to-air reversible heat pump, R454C appears to be the best alternative, while R455A showed good results for heating-only mode.
- For the replacement of R134a in a split heat pump water heater, R1234yf, R513A, and R450A demonstrated performances equivalent to those of R134a, although R450A exhibited slightly reduced thermal capacity.

Most of the alternative fluids belong to an A2L safety class due to their flammability, which implies a comprehensive study of risks, sizing, and compatibility.

While long-term alternatives exist for R407C and R134a with a GWP below 150, only transition alternatives are available for R410A. Hence, it is necessary to study other solutions, particularly natural fluids.

The latter segment of the project focuses on developing and manufacturing an R290 water-to-water heat pump prototype. The investigation yields noteworthy insights regarding the feasibility of crafting a 5 kW unit with less than 150 g of propane.

Numerous technical facets incorporated have a significant impact on charge reduction. Modifying the superheat and downsizing the plate evaporator helps to minimize the optimal charge. Using a semi-hermetic automotive compressor with a minimal oil quantity shows potential. Nonetheless, enhanced modeling encompassing the influence of oil and compressor capacity is imperative for optimizing the energy efficiency of the setup.